Abstract

GHOSH, RAHUL. Error analysis of Through Reflect Line method for calibrating microwave measurements. (Under the direction of Professor Michael B. Steer)

Uncertainty in transmission line based calibration techniques for microwave measurements are studied with the aim of identifying the optimum calibration conditions. Variation in the determined error parameters under certain conditions in Through Reflect Line (TRL) calibration method due to variation in the unknown reflection coefficient are analyzed experimentally and theoretically. It is found that measured uncertainty is minimized when the reflection standard is either a short or an open. The TRL calibration method is compared with the Through-Line (TL) calibration procedure. The major causes of uncertainties inherent in TRL calibration are absent in the TL calibration technique due to the synthesized reflection standard.

Error Analysis of the Through Reflect Line Method for Calibrating Microwave Measurements

By

Rahul Ghosh

A thesis submitted to the Graduate Faculty of
North Carolina State University
in partial fulfillment of the
requirements for the Degree of
Master of Science

Electrical Engineering

Raleigh

2003

Approved by:-

Prof. Gianluca Lazzi **Prof. Griff Bilbro**

_____ _____

Prof. Michael Steer, Chair of Advisory Committee

_____

Biographical Summary

Rahul Ghosh was born on 8th January 1979 in Calcutta, India. He received his elementary and secondary education in East Africa. He received the Bachelor of Science degree with a major in Electronics from on The Pune University, India, in 2000. From July 2000 until July 2001 he completed the Post-Graduate Diploma course in VLSI Design at Bitmapper Integration Technologies Pvt Ltd. In August 2001 he was admitted to North Carolina State University to study for the Master of Science in Electrical Engineering. His interest is in the field of hardware design.

Acknowledgements

I wish to express my appreciation to my advisor Dr. Michael Steer for his continuous support, guidance and hours of in-depth discussion that made this work possible. I would also like to thank Dr. Griff Bilbro and Dr. Gianluca Lazzi for serving on my committee. I would like to express my appreciation to Mr. Jayesh Nath and Mr. Mark Buff for their help and patience during the lengthy hours taking the measurements and clearing my doubts. My special thanks go to all of my other friends for their moral support and encouragement. And finally, I would like to express my gratitude to my past and present instructors who taught me and who provided me useful information about electrical engineering. This work is dedicated to my late father Aloy Kumar Ghosh.

Table of Contents

List of Figures

Chapter 1: Introduction

1.1 Motivation

The main motivation for this work is the recent development of a new technique, the Through Line (TL) calibration procedure developed by M. B. Steer, S. B. Goldberg, G. Rinnet, P. D. Franzon, I. Turlik and J. S. Kasten [1]. Under certain conditions this is a replacement for the Through-Reflect-Line (TRL) calibration procedure developed by G.F. Engen and C.A. Hoer [2]. Even though TRL is the most widely used calibration technique, this work tries to delve into the reasons why TL calibration appears to have better characteristics than the TRL calibration technique. In particular, the TRL procedure appears to have glitches when the length of the line standard is close to integer multiple of a half wavelength. These glitches are not apparent in TL calibration.

The TRL calibration technique suffers from inherent errors that result in uncertainties in the measurement when the phase delay along the line is a multiple of 180 degrees. The TL calibration also suffers from this inherent problem, but the reduced number of standards required in TL calibration is a major reason for better results as compared to TRL calibration. The Reflect standard for the TRL calibration need not be known accurately. This requirement makes the TRL calibration less susceptible to errors as compared to other calibration techniques like Through Short Delay (TSD) that requires the Reflection standard to be accurately known. This still does not guarantee that the TRL procedure is error free. In this work an error factor inherent in TRL calibration that is absent in TL calibration is found.

1.2 Thesis Overview

Chapter 2 presents a literature overview including brief introduction to the need for calibration in the microwave measurement. The basic operating principle of a vector network analyzer is discussed along with the different terminology associated with network analysis. Different types of errors and techniques of error correction applied to network analyzer measurements are discussed. The different error correcting calibration techniques are explained along with their inherent drawbacks and advantages. Chapter 3 discusses the TRL calibration procedure in detail as this calibration is the most popular and widely used for on-wafer measurements. The inherent errors in TRL calibration are discussed in details. Next the new calibration technique, TL calibration, is introduced and comparisons are made between the TRL and TL calibration methods. Chapter 4 discusses another possible inherent error, the variation in the reflection coefficient standard seen at the two ports of network analyzer that causes variation in the measured parameters for the error boxes in the TRL calibration and considerations to be made in selecting the Reflection standard to minimize these variations. Chapter 5 presents the experimental verification for the proposed error present in TRL. This includes MATLAB code implementing the TRL algorithm and the inherent errors introduced for different reflection co-efficient standards.

Chapter 2: Literature Review

2.1 Introduction to Smith Charts and VNA

This section gives an overview of the fundamental principles of vector network analysis and Smith Charts [7]. Network analyzers accurately measure ratios of the incident, reflected, and transmitted energy, e.g., the energy that is launched onto a transmission line, reflected back down the transmission line toward the source (due to impedances mismatch), and successfully transmitted to the terminating device. The amount of reflection that occurs when characterizing a device depends on the impedance that the incident signal "sees". This impedance can be represented by real and imaginary parts. Instead of plotting impedance directly, the complex reflection coefficient is displayed in vector form. The magnitude of the vector is the distance from the center of the display, and phase is displayed as the angle of vector referenced to a flat line from the center to the right-most edge. Smith charts are normally to represent this.

As mentioned in [8], Smith Chart is a polar plot of the complex reflection coefficient or also known as the 1-port scattering parameter S_{11}, for reflections from a normalized complex load impedance; the normalized impedance is a complex dimensionless quantity obtained by dividing the actual load impedance Z_L in ohms by the characteristic impedance Z_o (also in ohms, and a real quantity for a lossless line) of the transmission line. On the Smith Chart, loci of constant resistance appear as circles, while loci of constant reactance appear as arcs. Impedances on the Smith chart are always normalized to the characteristic impedance of the component or system of interest, usually 50 ohms for RF and microwave systems and 75 ohms for broadcast

and cable-television systems. A perfect termination appears in the center of the Smith chart.

2.1.1 Micro-strip device measurements

Microstrip devices cannot be connected directly to the coaxial ports of a network analyzer. The device under test (DUT) must be physically connected to the network analyzer by some kind of transition network or fixture. The Figure 2.1 below shows a typical block diagram of the different reference planes in microstrip device measurement.

In order to get the accurate measurement we need to remove all errors up to the fixture reference plane. This means that the internal Vector Network Analyzer (VNA) as well as coaxial cable errors must be removed. Calibration for a fixture measurement in micro-strip presents additional difficulties.

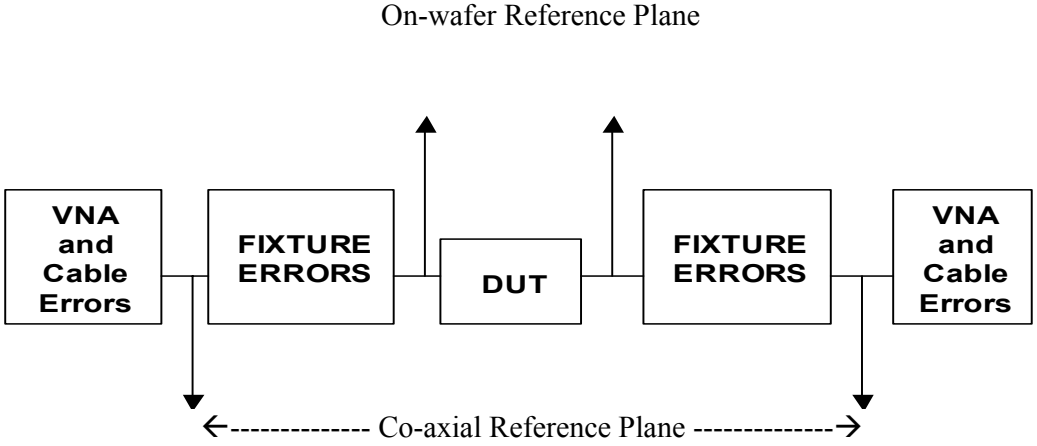

Figure 2.1: Reference planes in on-wafer microwave measurement.

Calibration at the coaxial ports of the network analyzer removes the effects of the network analyzer and any cables or adapters before the fixture; however, the

effects of the fixtures themselves are not accounted for. Thus calibration standards are required at the probe tips.

2.2 Measurement Errors

Errors in network analyzer measurements can be separated into three categories [9]:

1) **Systematic errors** are the most significant source of measurement uncertainty in RF and Microwave measurements, caused by imperfections in the test equipment and test setup. These errors can be characterized through calibration and mathematically removed during the measurement process. Systematic errors encountered in network measurements are related to signal leakage, signal reflections, and frequency response. The six systematic errors in the forward direction are directivity, source match, reflection tracking, load match, transmission tracking, and isolation. The reverse error model is a mirror image, giving a total of 12 error terms for two-port measurements.

2) **Drift errors** occur when a test system's performance changes after a calibration has been performed. They are primarily caused by temperature variation and can be removed by additional calibration.

3) **Random errors** vary as a function of time. Since they are not predictable they cannot be removed by calibration. The main contributors to random errors are instrument noise, switch repeatability, and connector repeatability.

2.2.1 Error Correction Techniques

Vector error correction [9] is the most widely used approach to removing systematic errors. This type of error correction requires a network analyzer capable of measuring

phase as well as magnitude, and a set of calibration standards with known, precise electrical characteristics. The vector-correction process characterizes systematic error terms by measuring known calibration standards, storing these measurements within the analyzer's or controller's memory, and using this data to calculate an error model which is then used to remove the effects of systematic errors from subsequent measurements. This calibration process accounts for all major sources of systematic errors and permits very accurate measurements. However, measurement accuracy is largely dependent upon calibration standards, and a set of calibration standards is often supplied as a calibration kit.

2.3 Measurement Calibration Standards

The two main types of vector error correction are the one-port and two-port calibrations.

2.3.1 One Port Calibration

This procedure consists of measuring a series of known calibration standards. Based on the measurements of these known standards, an error model of the performance characteristics of the microwave hardware internal to the network analyzer can be constructed. After this error model has been generated from the measurement of the calibration standards, the network analyzer removes the systematic errors from the other devices.

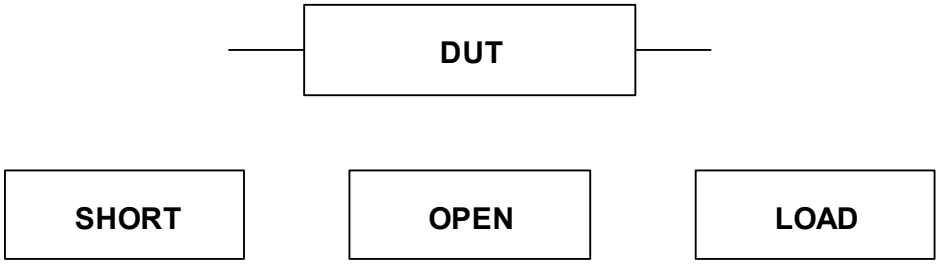

Figure 2.2: One port OSL calibration standards.

The three standards used for 1-port calibration are the short, open, and matched termination as shown in Figure 2.2. Based on the measurements made for each of these standards, the values of the components in the systematic error model (e00, e01 and e11), as shown in Figure 2.3, can be computed. Once these values are found, the S parameters of the DUT can be corrected for these non-idealities.

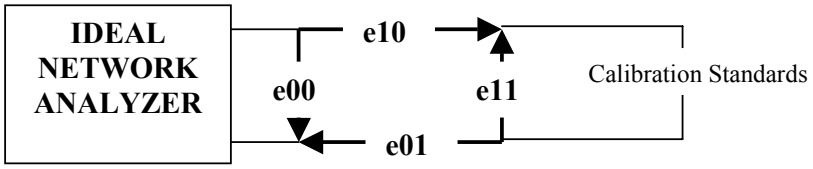

Figure 2.3: One port error model.

In the error model

e00 is the Directivity error

e01, e10 are the Reflection error

e11 is the Source Match error

This method is generally used for reflection measurements. The method needs good termination for high accuracy with two-port devices.

2.3.2 Two Port Calibration

In calibrating a two-port device however, one port calibration assumes a good termination on the unused port of the DUT. This may cause inaccuracies if the unused port of the DUT is not perfectly matched. To obtain highest accuracy two-port error correction is used. The two-port error correction yields the most accurate results because it account for all of the major sources of systematic error. The error model shown in Figure 2.4 for a two-port device reveals the four S-parameters measured in the forward and reverse directions. Once the system error terms have been characterized, the network analyzer utilizes four equations to derive the actual device S-parameters from the measured S-parameters. Because each S-parameter is a function of all four measured S-parameters, a network analyzer must make a forward and reverse test sweep before updating any one S-parameter.

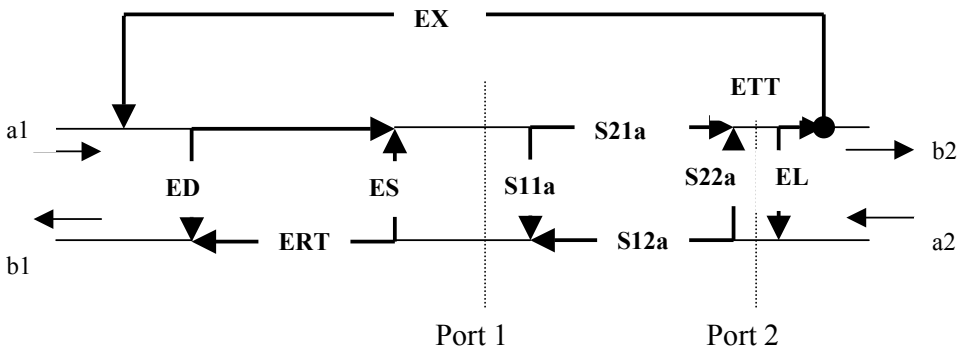

Figure 2.4: Two port forward error model.

In the error model:

ED is the Forward Directivity error
ES is the Forward Source Match error
ERT is the Forward Reflection Tracking error
EL is the Forward Load Match error
ETT is the Forward Transmission Tracking error
EX is the Forward Isolation error

The most commonly used two-port calibration techniques are:

Short Open Load Through (SOLT)

Through Short Delay (TSD)

Through Reflect Line (TRL)

Line Reflect Match (LRM)

And Through Line (TL)

These calibration techniques are described in the sections below.

2.3.2.1 Short Open Load Through (SOLT) Calibration

Calibration at the coaxial ports of the network analyzer removes the effect of the network analyzer and any other cable before the fixture. Most network analyzers already contain standard calibration kit definition files that describe the characteristics of a variety of calibration standards. These calibration kit definitions usually cover the major types of coaxial connectors used for component and circuit measurements.
This method is simpler and very accurate as long as the standards are accurately defined.

The SOLT calibration technique is often preferred when S-parameters are measured with respect to an ideal characteristic impedance such as 50 ohm. Main characteristics of Short Open Load Though Calibration are that all standards open, short, load must be perfectly known. The open standard is typically realized as an unterminated transmission line. Electrical definition of an ideal open has unity reflection with no phase shift. The actual model for the open, however, does have some phase shift due to fringing capacitance. The electrical definition of an ideal short is unity reflection with 180 degrees of phase shift. All of the incident energy is reflected back to the source, perfectly out of phase with the reference. A simple short

circuit from a single conductor to ground makes a good short standard. For example, the short can be vias (plated through holes) to ground at the end of a micro-strip transmission line. If coplanar transmission lines are used, the short should go to both ground planes. To reduce the inductance of the short, avoid excessive length. A good RF ground should be near the signal trace. An ideal load reflects none of the incident signal, thereby providing a perfect termination over a broad frequency range. We can only approximate an ideal load with a real termination because some reflection always occurs at some frequency, especially with non-coaxial actual standards.

2.3.2.2 Through Short Delay (TSD) calibration

TSD was developed by N. R. Franzen and R. A. Spaciale [11] and is based on both reflection and transmission measurements and it offers two advantages. First, a matched load standard in not required and second it uses mechanically simple standards. TSD is not without disadvantage. The delay standard is assumed lossless and nonreflecting i.e. the propagation constant was pure delay and the impedance was the measurement system or 50 ohms. Also, TSD requires information from two delays; the through connection and the actual delay. If the phase difference between these two is near zero or 180 degrees the algorithm fails to return a valid result. This is a limitation of any de-embedding technique using a delay type standard.

2.3.2.3 Through Reflect Line (TRL) Calibration

For in-fixture calibration high quality Short-Open-Load-Thru (SOLT) standards are not readily available for full 2-port calibration of the system at the desired measurement plane of the device. In microstrip, a practical short circuit or via is inductive, a practical open circuit radiates energy and a high-quality purely resistive

load is difficult to produce over a broad frequency range. TRL Calibration as developed by Engen and Hoer [1], used only one delay standard with a through connection and an arbitrary reflection to calibrate their network analyzer. The delay standard could be arbitrary, with its propagation constant unknown, however, the line was assumed nonreflecting. The reflection standard could be any repeatable reflecting load and they suggested either an open or short circuit. The Through Reflect Line (TRL) 2-port calibration is an alternative to the traditional SOLT full 2-port calibration technique that utilizes simpler more convenient standards, for device measurements in the microstrip environment.

The TRL method is more suitable for obtaining S-parameters with respect to the impedance of on wafer transmission lines. When accurate on-wafer Line standards are available, the TRL method usually offers better accuracy than the SOLT technique. A TRL 2-port calibration kit uses at least three standards to define the calibrated reference plane. For TRL two port calibrations, the 12 terms error model as introduced earlier is simplified to eight terms error model as shown in Figure 2.5. A total of 10 measurements are made to quantify the eight unknowns.

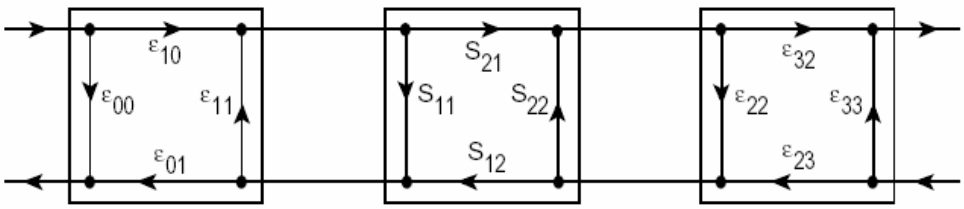

Figure 2.5: Modified eight term error model [12].

In the error model
ε00 is the Forward Directivity error
Product of ε10 and ε01 is the Reflection Tracking error
ε11 is the Load and Source Match error
Product of ε10 and ε32 is the Transmission Tracking error

An assumption is made that:

ε11 = Forward Source Match error = Reverse Load Match error.

ε22 = Reverse Source Match error = Forward Load Match error.

The main characteristic of Though Reflect Line Calibration are that the TRL technique requires only a through-line (Through) and a transmission line offset (Line) as references. The TRL method also employs highly reflecting impedances (Reflects) as standards, but their exact electrical characteristics are not required. However, Reflect standards must be accurately repeated at each test port. The TRL calibration uses the characteristic impedance of the length of the transmission line standard to set the reference impedance. This approach restricts the range of frequency that can be measured as the insertion phase of the line should lie between 20 and 160 degrees. Because of this reason, most of the Line standards can only be used over an 8:l frequency range. For broadband measurements several Line standards may be required. At low frequencies, Line standards can become inconveniently long. Another concern is the change of the reference impedance due to the effects of loss and dispersion in the TRL Line standards. The accuracy of the method depends on the estimate of the characteristic impedance of the Line standard.

2.3.2.4 Load Reflect Match (LRM) Calibration

The standards for the LRM calibration method are a non-zero length Through line, a Reflect and a Match. The LRM calibration method is similar to the TRL calibration method, except that a perfect match on each port is substituted in place of the Line standard. The matched standard can be seen as an infinitely long line. The LRM

reflect is the same as the TRL reflect standard, the value of the reflection standard need not be known accurately, but must be the same for each port. The LRM Line standard corresponds to the TRL Through standard.

The LRM calibration offers a number of advantages. Firstly, the Matched standard is the only impedance that needs to be accurately known thereby reducing the errors caused by improperly defined open or short standards used in SOLT calibration method. The advantage over the SOLT calibration lies in the fact that LRM calibration uses lesser standards that results in fewer standard definitions and the errors resulting from imperfect standard definition are minimized. Secondly, the use of Matched standard to determine the reference impedance reduces the variation in the reference impedance value as observed in TRL method and enables broadband frequency coverage.

2.3.2.5 Through Line Calibration

The Through Line (TL) calibration is a two tier calibration procedure. The TL method utilizes measurements of the through and line following approximate Open Short Line calibration. The Through Line calibration is implemented in three steps. The first step is to apply Open Short Load (OSL) calibration to each of the two test ports. The only requirement for the OSL calibration is that the same reference impedance be used at the two test ports. The second step is to perform the through and line measurements. The through measurement yields the reflection coefficient of an ideal short placed at the fixture reference plane. This removes the need for arbitrary reflection standard as in TRL procedure thus removing the major source of ambiguity.

Figure 2.6 below shows the conventional two port error network and its corresponding signal flow graph. It is composed of two error networks A and B where the individual signal paths S_{ija} and S_{ijb} are unique forcing the fixture S parameters S_{ijf} to be unequal to each other. This represents an asymmetric fixture. As explained in [13], the fixture is symmetric if the port 1 and 2 reflection coefficients are equal and the fixture is reciprocal, i.e. if $S_{11f} = S_{22f}$ and $S_{21f} = S_{12f}$. Reciprocity is true when the fixture is passive and non-magnetic and these symmetrical equalities are possible with two orders of symmetry; first and second order.

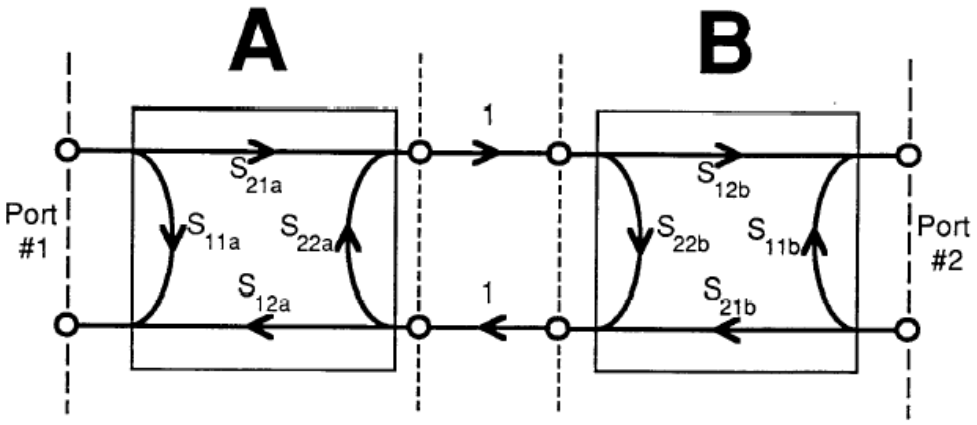

Figure 2.6: Two port error model for asymmetric fixtures [13].

From the signal flow graph of the asymmetric fixtures in Figure 2.6, applying Mason's rule yields

$$S_{11f} = S_{11a} + \frac{S_{21a}S_{12a}S_{11b}}{1 - S_{22a}S_{11b}} \tag{2.1}$$

$$S_{22f} = S_{22b} + \frac{S_{22a}S_{21b}S_{12b}}{1 - S_{22a}S_{11b}} \tag{2.2}$$

$$S_{21f} = \frac{S_{21a}S_{21b}}{1 - S_{22a}S_{11b}} \tag{2.3}$$

And

$$S_{12f} = \frac{S_{12a}S_{12b}}{1 - S_{22a}S_{11b}} \tag{2.4}$$

From equation 2.1 and 2.2 we get

$$S_{11a}(1 - S_{22a}S_{11b}) + S_{11b}S^2_{21a} = S_{22b}(1 - S_{22a}S_{11b}) + S_{11b}S^2_{21a} \tag{2.5}$$

As a result of approximate OSL calibration, the calibrated fixtures of the test system are identical. Hence in a through connection the embedded device under test is symmetrical. Symmetry permits the synthesis of TRL reflection standards. A first-order symmetric fixture has identical fixture halves that are symmetric as shown in Figure 2.7. The port two error network, B, is now a port reverse of A, or $B = A^R$. This is true if $S_{lla} = S_{22b}$, $S_{22a} = S_{llb}$. Moreover, these conditions satisfy the symmetry condition equation (2.5). Most importantly, the signal flow graph in Figure 2.8 shows symmetry reduces the number of error terms to three, the A network only. In other words, symmetry reduces the number of error terms for a two port fixture.

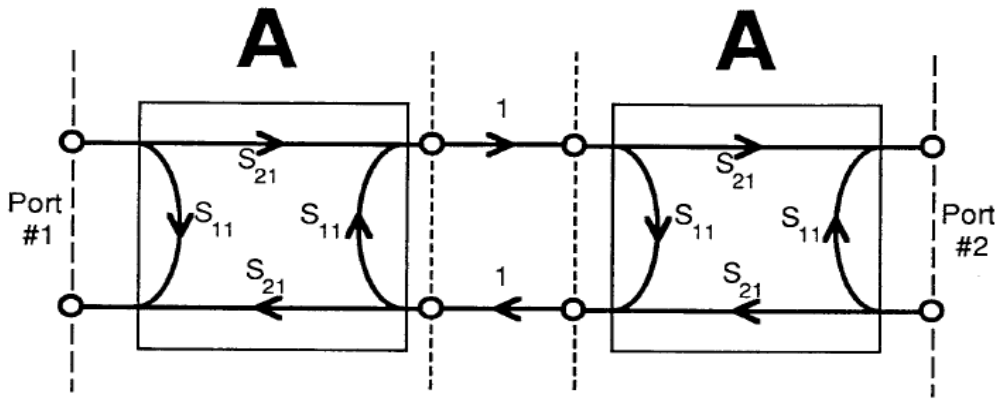

Figure 2.7: Reduced two port error model for symmetric fixtures [13].

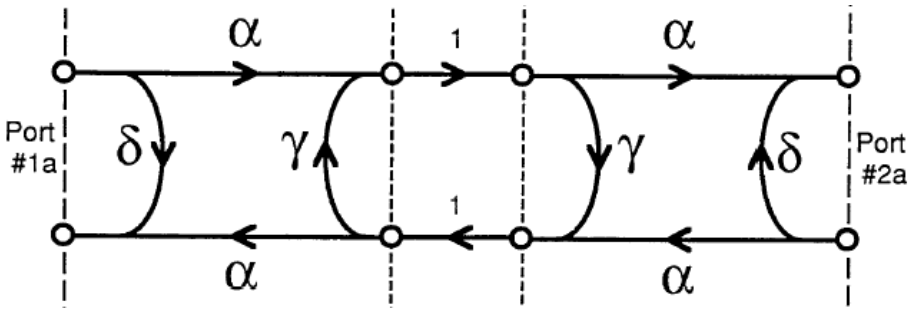

Figure 2.8: Signal flow graph of reduced two port error model for symmetric fixtures.

Synthesize Reflection Standards

In the signal flow graphs of Figure 2.9, we consider the through connection S parameters given by S_{llf} (= S_{22f}) and S_{21f} (= S_{12f}), and the actual parameters of the error network A being δ, α, γ (for S_{lla}, S_{21a} = S_{12a} and S_{22a} respectively).

In addition, the input reflection coefficient with an ideal short circuit placed at port 1b of A is

$$\rho_{sc} = \delta - \alpha^2/(1-\gamma) \qquad (2.6)$$

From the signal flow graphs we obtain

$$S_{llf} = \delta + \alpha^2 \gamma /(1-\gamma^2) \qquad (2.7)$$

$$S_{21f} = \alpha^2/(1-\gamma^2) \qquad (2.8)$$

From (2.6), (2.7) and (2.8) we get

$$\rho_{sc} = S_{llf} - S_{21f} \qquad (2.9)$$

Similar results hold for

$$\rho_{oc} = S_{llf} + S_{21f} \qquad (2.10)$$

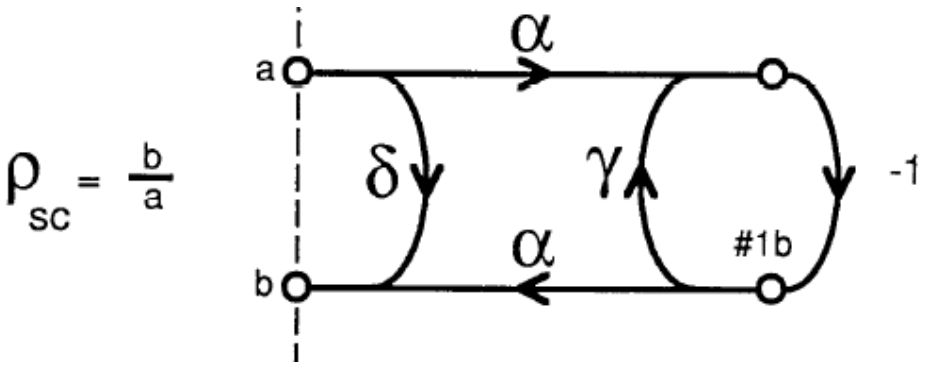

Figure 2.9: Signal flow graph of ideal short as reflection coefficient.

Compared to TRL, TL calibration reduces the number of standards needed and requires fewer connections to the microstrip ports improving the repeatability of this connection. Since the reflection coefficients are derived mathematically, it is possible to "insert" ideal open and short circuits within a non-insert able medium such as a dielectric loaded waveguide. The TL procedure also determines the frequency dependent characteristic impedance of the line standard. The characteristic impedance of the line standard is determined from the scattering parameter measurements and the measured free space capacitance of the reference line. Hence the two tier calibration along with the frequency dependent characteristic impedance of the line standard avoids the periodic glitches inherent in the TRL procedure.

2.4 Conclusion

This chapter discussed the different types of errors introduced in microwave measurements and the calibration techniques available to remove these errors. The one port and two port error correction techniques are introduced along with their respective error models and the limitations of one port error model were stated. A brief overview of the popular two port error correction methods are discussed along

with their advantages and disadvantages. In the next chapter the Through Reflect Line calibration is discussed in detail along with the derivation of the TRL algorithm.

Chapter 3: TRL Calibration

This chapter discusses the TRL calibration technique [3] in depth and analyzes the different steps involved in this calibration and why this method is the most popular of all. The inherent advantage of TRL calibration as compared to all other calibration techniques discussed so far is that the value of the reflection standard need not be known. The main features of TRL calibration have already been discussed in the previous chapter. In this chapter the mathematical analysis of the TRL deembedding procedure is presented as this is necessary to understand the proposed inherent error introduced due to the arbitrary reflection coefficient.

3.1 Steps in TRL Calibration

For the 'thru' step, the test ports are connected together directly (zero length thru) or with a short length of transmission line (non-zero length thru). The transmission frequency response and port match are measured in both directions by measuring all four S-parameters. For the 'reflect' step, identical high reflection coefficient standards (typically open or short circuits) are connected to each test port and measured (S_{11} and S_{22}). For the 'line' step, a short length of transmission line different in length from the THRU) is inserted between port 1 and port 2 and again the frequency response and port match are measured in both directions by measuring all four S-parameters. In total, ten measurements are made, resulting in ten independent equations. However, the TRL error model has only eight error terms to solve for. The 'reflect' standard and the propagation constant of the 'line' standard are determined. Because these terms are solved for, they do not have to be specified initially. The

characteristic impedance of the 'line' standard becomes the measurement reference and, therefore, has to be assumed ideal (or known and defined precisely).

3.2 TRL De-Embedding Solution

The basic TRL calibration outlined in [1] is based on the eight term error model. The procedure then consists of finding the S parameters for the two two-port error matrices. A more detailed derivation of the TRL calibration equations is given in Appendix A. The set of measurements for the uncalibrated S parameter of the DUT can be written in terms of R (T parameters) matrices as:

$$R_M = R_a * R_{DUT} * R_b$$

where R_M represents the measured T matrix, R_{DUT} represents the actual T matrix of the DUT (Device Under Test) and R_a and R_b are the error box T matrices. Once the calibration is complete and the terms of the error matrices determined, the T parameters of the DUT can be easily determined from

$$R_{DUT} = inv(R_a) * R_M * inv(R_b)$$

where 'inv' is the matrix inverse.

This results in explicit expressions for the de-embedded S parameters.

The calibration procedure consists of measuring the S matrices for the three standards, namely Thru, Reflect and Line, which gives three known matrices. The three matrices obtained give the scattering parameters of the fictitious two ports as shown in the Figure 3.1 in the next page and the scattering parameters of the individual error boxes A and B.

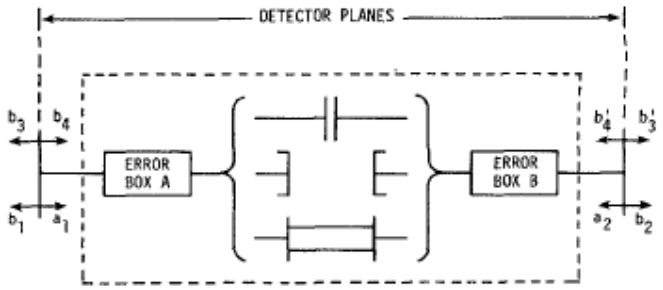

Figure 3.1: Fictitious two-port error boxes A, B with the three standards. [3]

The emergent wave amplitudes $\mathbf{b}_1$, $\mathbf{b}_2$ at ports 1 and 2 are related to the incident waves $\mathbf{a}_1$, $\mathbf{a}_2$ by the well-known scattering equations:

$$b_1 = S_{11}a_1 + S_{12}b_2 \tag{3.1}$$

$$b_2 = S_{21}a_1 + S_{22}b_2 \tag{3.2}$$

where the S_{ij} are the scattering coefficients.

Dividing the first of these by $\mathbf{a}_1$, the second by $\mathbf{a}_2$, and then eliminating the ratio $\mathbf{a}_1/\mathbf{a}_2$ between them yields:

$$w_2S_{11} + w_2S_{22} - \Delta = w_1w_2 \tag{3.3}$$

where

$$\Delta = S_{11}S_{22} - S_{12}S_{21} \tag{3.4}$$

Equation (3.5) shows the conversion between the T and the S parameters.

$$\begin{bmatrix} R_{11} & R_{12} \\ R_{21} & R_{22} \end{bmatrix} = \begin{bmatrix} -\dfrac{S_{11}S_{22} - S_{12}S_{11}}{S_{21}} & \dfrac{S_{11}}{S_{21}} \\ -\dfrac{S_{22}}{S_{21}} & \dfrac{1}{S_{21}} \end{bmatrix} \tag{3.5}$$

First convert the measured S parameters to their equivalent T parameters as in Equation (3.5). Let the cascading matrix be represented by the matrix **R**. Let the

cascading matrices of the error two-ports **A** and **B** be denoted by $\mathbf{R}_a$ and $\mathbf{R}_b$ respectively, while R_t represents their cascade 'thru' connection and R_d represents the cascade 'Line' measurements and R_{l1} represents the cascade matrix of the inserted line.

The T matrix for the Though connection can be represented by

$$R_t = R_a R_b \tag{3.6}$$

while the T matrix for the line connection can be represented by

$$R_d = R_a R_{l1} R_b \tag{3.7}$$

where

R_a matrix be represented by: $\mathbf{R}_a = \begin{bmatrix} r_{11a} & r_{12a} \\ r_{21a} & r_{22a} \end{bmatrix}$

or $\mathbf{R}_a = r_{22a} \begin{bmatrix} a & b \\ c & 1 \end{bmatrix}$

$a = r_{11a} / r_{22a}$, $b = r_{12a} / r_{22a}$ and $c = r_{21a} / r_{22a}$.

R_b matrix be represented by: $\mathbf{R}_b = \begin{bmatrix} r_{11b} & r_{12b} \\ r_{21b} & r_{22b} \end{bmatrix}$

or $\mathbf{R}_b = r_{22b} \begin{bmatrix} \alpha & \beta \\ \gamma & 1 \end{bmatrix}$

$\alpha = r_{11b} / r_{22b}$, $\beta = r_{12b} / r_{22b}$ and $\gamma = r_{21b} / r_{22b}$.

Solving equation (3.6) for $\mathbf{R}_b$ and substituting into equation (3.7) gives

$$TR_a = R_a R_{l2} \text{ where } T = R_d \, R_t^{-1} \tag{3.9}$$

The equation (3.9) consists of four equations with five unknowns. However there are only three independent solutions to Equation (3.9). These solutions give

$a / c = (r_{11a} / r_{21a})$, $b = (r_{12a} / r_{22a})$

and $e\exp(2\gamma\ell) = \dfrac{t_{21a}(r_{12a}/r_{22a}) + t_{22a}}{t_{12a}(r_{21a}/r_{11a}) + t_{11a}}$. (3.10)

Up to this step we have solved for two terms of the error matrix **A** and the propagation constant of the transmission line. Using this information we can solve for $\mathbf{R}_b$ using equation (3.6) to obtain two parameters of the error matrix **B** namely β/α and γ.

Next we make use of the reflection standard. The reflection coefficient measured at port 1, w_1, can be written as a function of the reflection coefficient of the termination Γ_l and the S parameters of the error box A as

$$w_1 = \frac{a\Gamma_l + b}{c\Gamma_l + 1} \tag{3.24}$$

or

$$a = \frac{w_1 - b}{\Gamma_l(1 - w_1 * c/a)} \tag{3.25}$$

Similarly, we can write for the measured reflection coefficient at the error box B as

$$w_2 = \frac{\alpha\Gamma_l - \gamma}{-\beta\Gamma_l + 1} \tag{3.26}$$

or

$$\alpha = \frac{w_2 - \gamma}{\Gamma_l(1 + w_2 * \beta/\alpha)}. \tag{3.27}$$

The unknown reflection coefficient Γ_l is eliminated from Equation (3.25) and (3.27) to yield

$$a = \pm\sqrt{[(w_1 - b)(1 + w_2\beta/\alpha)(d - bf)]/[(w_2 + \gamma c/a)(1 - ec/a)]} \tag{3.28}$$

Thus the need for the value of reflection coefficient to be exactly known is eliminated. Once the value for 'a' for two port error matrix A is found, the remaining parameters of the error matrix A and B can be easily found as

$$\gamma = \frac{f - dc/a}{1 - ec/a} \tag{3.30}$$

$$\frac{\beta}{\alpha} = \frac{e - b}{d - bf} \tag{3.31}$$

$$a\alpha = \frac{d - bf}{1 - ec/a} \tag{3.32}$$

At this point the TRL calibration development is complete. The S parameters of the error matrix **A** are given in terms of the measured quantities by:

$$S_{11A} = b = \frac{r_{12a}}{r_{22a}} \tag{3.33}$$

$$S_{22A} = \frac{r_{21a}}{r_{22a}} = -\frac{r_{21a}}{r_{11a}}\frac{r_{11a}}{r_{22a}} = -\frac{c}{a} * a \tag{3.34}$$

$$S_{12A} * S_{21A} = \frac{r_{11a}}{r_{22a}}\left\{ 1 - \left(\frac{r_{12a}}{r_{22a}}\right)\left(\frac{r_{21a}}{r_{11a}}\right) \right\} = a\left\{ 1 - b * c/a \right\} \tag{3.35}$$

As is evident from the above equations, the TRL calibration solves only for the error matrix product $S_{12A} * S_{21A}$. The reasons behind the popularity of the TRL algorithm as compared to the other two port calibration techniques, namely SOLT (Short Open Load Through) calibration, OSL (Open Short Load) calibration and TSD (Through Short Delay) calibration are: Firstly the TRL calibration does not need Short and Open standards. These standards limit the accuracy of the measurement, as the values of these standards need to be accurately known to determine the error parameters. Secondly the most important advantage of the TRL algorithm is the value of the Reflect standards used for calibration need not be known to determine the parameters of the error matrix. Thus the calibration procedure is not dependent on the accurate determination of the standards used. Hence the TRL calibration procedure is still the most popular and widely used calibration procedure. However the TRL calibration is

not without its drawbacks. In the following section some of the drawbacks of the TRL calibration procedure are discussed.

3.3 Limitations of Thru-reflect line (TRL) Calibration

The major limitation of the TRL technique is the limited bandwidth of Line standards. Most Line standards can only be used over a limited frequency range. For broadband measurements, several Line standards may be required. At low frequencies, Line standards can become inconveniently long.

The algorithm requires the characteristic impedance of the line standard be equal to the measurement system impedance. If not, its value has to be determined. Also, the algorithm assumes real characteristic impedance with no frequency dependence. If the fixture to be calibrated is composed of dispersive transmission lines, e.g. microstrip, it becomes necessary to determine the complex characteristic impedance as a function of frequency.

The insertion phase of the line must not be same as the thru (for zero or non-zero length). This puts an important requirement that the difference between the length of the Line standard (say l_2 and the length of the thru standard (say l_1 must be between (20º and 160º) ± n×180º. Ideally the difference between the lengths is taken to be ¼ wavelength or 90º of the insertion phase relative to the thru at the middle of the desired frequency span. Hence the range of frequencies over which the measurements are to be taken decides the center frequency, which in turn decides the difference between the two lengths.

3.4 Conclusion

This chapter discussed in detail the TRL calibration procedure. The discussion included the requirements of the standards used in the TRL calibration, the mathematical analysis of the TRL de-embedding algorithm, the advantages of this calibration procedure as compared to the other two port calibration methods. In the end the inherent drawbacks and limitations of this popular procedure are discussed.

Chapter 4: Error Analysis of TRL Calibration

This chapter presents the reader with the new work done to investigate why the TL (Through Line) calibration, under certain conditions provides a better alternative to the TRL (Through Reflect Line) calibration. In the following sections the discrepancies introduced in the calculated parameters of the error matrices due to the arbitrary reflection standard is derived. The inherent assumption about the reflection standard value in the TRL de-embedding algorithm is seen to cause variations in the obtained parameters of the error matrices. From the derivation of this error factor, the uncertainties are found to be dependent on the value of the selected arbitrary reflection standard. Another phenomenon, namely the discrepancies in measurement when the line difference approaches an integer multiple of a half wavelengths, is also observed in TL calibration technique. Mathematical analysis is presented to indicate the cause of these discrepancies in the TL and TRL calibration and the conclusion is drawn that the discrepancies will be observed in all calibration procedure that uses the through and delay standards as part of the calibration procedure.

4.1 Proposed Error in TRL calibration

There have been a number of papers investigating the various causes of error inherent in TRL calibration. Marks [16] uses least mean square estimate and redundant transmission line standards to minimize the effects of random errors introduced by imperfect connector repeatability. The measured model in this paper is represented by cascade of the fixture error matrices and the transmission line matrix. The fixtures

used are assumed to be symmetric and represents the error cascade matrix $\begin{pmatrix} \alpha & \beta \\ \gamma & \delta \end{pmatrix}$ and its reverse cascade matrix as $\begin{pmatrix} \delta & \gamma \\ \beta & \alpha \end{pmatrix}$. In order to take into consideration the errors introduced in the measurement due to imperfection in the transmission lines, the transmission line matrix is further represented as cascade of three matrices $\mathbf{T}i = [I + \delta 1i]\ \mathbf{L}_i\ [I + \delta 2i]$ where $\mathbf{L}_i$ represents the ideal error free transmission line matrix and δ represents the imperfections in transmission line and the error is assumed to be small. The two set of measurements taken are represented by the two matrices as $\mathbf{M}_i = \mathbf{X}\ \mathbf{T}_i\ \mathbf{Y}_b$ and $\mathbf{M}_j = \mathbf{X}\ \mathbf{T}_j\ \mathbf{Y}_b$ where $\mathbf{X}$ represents the first error matrix of the fixture and $\mathbf{Y}_b$ represents the reverse cascade error matrix. Solving the two set of equations to eliminate $\mathbf{Y}_b$ results in $\mathbf{M}_{ij}\mathbf{X} = \mathbf{X}\ \mathbf{T}_{ij}$ where $\mathbf{M}_{ij} = \mathbf{M}_j\ * \mathbf{M}_i^{-1}$ and $\mathbf{T}_{ij} = \mathbf{T}_j\ * \mathbf{T}_i^{-1}$. Since the matrices $\mathbf{M}_{ij}$ and $\mathbf{T}_{ij}$ have identical eigen values, the effect of perturbations on matrix M_{ij} can be analyzed via their effects on $\mathbf{T}_{ij}$. The mathematical analysis that follows in the paper results in the transmission line matrix represented by $\mathbf{T}_{ij} \approx \mathbf{L}_{ij} + \varepsilon_{ij}$ where ε_{ij} is the linear difference term, $\mathbf{L}_{ij} = \mathbf{L}_j\,\mathbf{L}_i^{-1} = \begin{bmatrix} E1 & 0 \\ 0 & E2 \end{bmatrix}$

E1= $e \exp[-\gamma(\ell 1 - \ell 2)]$ and E2 = $e \exp[+\gamma(\ell 1 - \ell 2)]$. The off diagonal elements of the error term ε_{ij} represents the errors in measurement of the reflection coefficient of the line and the diagonal elements represent errors in the measurement of the transmission coefficients of the line. The error term ε_{ij} vanishes when the transmission line is lossless and error free. The error analysis done in this work estimates the discrepancies in the TRL measurements caused due to losses in the transmission line standards and applies the least mean square algorithm to estimate the variation in the propagation constant γ based on the ε_{ij} error matrices.

Hoer [15] discusses the systematic error in measuring the reflection coefficient at a single port. To determine the systematic errors introduced, the reflection coefficient is measured for different combinations of attenuator connected with different reflection standard of values ($|\Gamma\ell|$) equal to 0.01, 0.05, 0.1 and 1.0. These measured reflection coefficient Γ_m are then compared with the reflection coefficient calculated from the individually measured S parameters of the different attenuators used and the reflection standards ($|\Gamma\ell|$) used for the measurements from the signal flow graph as $\Gamma_c = S_{11} + \frac{S_{12}S_{21}\Gamma_\ell}{1 - S_{22}\Gamma_\ell}$. The difference between the measured value $|\Gamma_m|$ and the calculated value $|\Gamma_c|$ is an indication of the systematic errors introduced.

Williams and Marks [18] analyze the bounds on the variations in the measured S parameters introduced due to the differences in the reference impedance or the reference plane. The measured cascade matrix is modified to take into account the adjusted reference impedance or the reference plane. Hence the cascaded matrix of $T_M = X_o\ T_o\ Y_{ob}$ is modified, to take into account the variation due to the reference impedance, to $T_M = [X_o\ R(Z,\ l)]\ T_o\ [Y_{ob}\ R(Z,\ l)_b]$ where the error matrices are represented by X_o and Y_{ob} and

$R(Z,\ l) \equiv \frac{1}{\sqrt{1 - \Gamma \exp 2}} \begin{bmatrix} e\exp[-\gamma(\ell - \ell o)] & \Gamma(e\exp[-\gamma(\ell - \ell_o)]) \\ \Gamma(e\exp[\gamma(\ell - \ell_o)]) & e\exp[\gamma(\ell - \ell_o)] \end{bmatrix}$ represents the variations when the reference plane changes to ℓ or the reference impedance changes to Z and $\Gamma = \frac{Z - Z_o}{Z + Z_o}$. The worst-case deviations of the measured S parameters and the impedance and reference plane transformed S parameters are derived to be

$B \le |\delta x_{11} - \delta x_{22}| + 2|\delta x_{21}| + |\delta x_{12}| + |\delta y_{21}|$

where $\delta x = [X_o\, R\, (Z, l)] - I$ and $\delta y = [Y_o\, R\, (Z, l)] - I$. This result shows the variation between the measured and the actual S parameters of the DUT for change in the reference impedance or the reference plane.

Kaiser and Williams [17] analyse different sources of systematic errors in the coplanar waveguide TRL calibration. Among the sources of systematic errors analyzed, the asymmetry in the symmetric short standard is also considered. The paper makes use of the result $B = |T_{11} - T_{22}| + 2|T_{21}| + |T_{12}|$ derived by Williams and Marks [18] to establish maximum variation between the measured and the actual S parameters when the short standard seen at one port has an offset of $\Delta\ell$. The upper bound of the error is seen to be directly proportional to the amount of offset $\Delta\ell$. The analyses done in [17] and [18] establish the discrepancies caused in the TRL calibration due to change in the reference plane and offset in the short standard.

Summarizing the work done to estimate the sources of error in TRL calibration due to the variation in the reflection coefficient standard includes work by Marks [16] that estimates the errors due to the losses in the transmission line standard, work by Hoer [15] that estimates the systematic errors introduced at a single port by the reflection coefficient standard and the work by Williams and Marks [18] and Kaiser and Williams [17] that estimates the errors due to the change in the reference plane and offset in the short standard. In the following section another new source of error due to the arbitrary reflection standard is introduced, mathematically derived and its implications discussed.

4.1.1 Analysis of the proposed inherent Error in TRL Calibration

This section introduces the proposed errors introduced in the TRL measurements due to the arbitrary reflection standard. With reference to [1], the TRL calibration does not assume symmetric and identical fixtures and hence has different error matrices for both the fixtures that increases the number of standards needed to find the parameters of the error matrices. The TRL calibration de-embedding procedure by Engen and Hoer [1] makes use of three standards, the through, an arbitrary reflection standard whose value need not be known, and a length of transmission line to de-embed the parameters of the error boxes. The through and the line standards yield two set of equations that are solved to find the propagation constant and two parameters of one of the error matrix. In the next step, the two set of measurements obtained by connecting the unknown reflection standard at the two ports are solved simultaneously to eliminate the unknown reflection standard and hence making the TRL de-embedding procedure independent of the unknown reflection standard value.

In the TRL de-embedding procedure an important assumption has been inherently made, namely that the reflection standard seen at the two ports is exactly same. This assumption cannot be overlooked as based on this assumption the two sets of measurements, obtained by connecting the unknown reflection standard at the two ports, are simultaneously solved to eliminate the unknown reflection standard. Hence for the TRL de-embedding procedure to be accurate, the unknown reflection standard seen at the two ports have to be exactly same.

In the following sections analysis is done to see the implications on the obtained parameters of the error matrices if the reflection standard seen at the two ports is not exactly same. Let us assume that the arbitrary reflection standard used in the TRL calibration procedure suffers from repeatability errors and the unknown

reflection standard seen at the two ports are not exactly the same value. Let the reflection standard seen at one port be Γ_l and the reflection standard value seen at the other port be $(\Gamma_l + \varepsilon)$. From the TRL de-embedding procedure mentioned in the derivation in chapter 3 and in Appendix A, the modified TRL de-embedding procedure is presented below.

With the modified reflection standard $(\Gamma_l + \varepsilon)$ seen at port 2, Equation (A.27), identical to Equation (3.27), is modified from $\alpha = \dfrac{w_2 - \gamma}{\Gamma_l(1 + w_2 * \beta / \alpha)}$ to

$\alpha = \dfrac{w_2 - \gamma}{(\Gamma_l + \varepsilon) * (1 + w_2 * \beta / \alpha)}$. Note that the only modification is that the reflection standard Γ_l is replaced with $(\Gamma_l + \varepsilon)$ where the term ε shows the variation in the reflection standard value, as seen at port 2 of the network analyzer, relative to the reflection standard presented at port 1. Equation (A.25), identical to Equation (3.27) remains unchanged as $a = \dfrac{w_1 - b}{\Gamma_l(1 - w_1 * c / a)}$ as this only depend on the reflection standard connected at port 1, and this remains unchanged. The next step in the TRL de-embedding algorithm eliminates the reflection standard by taking ratio of $\dfrac{a}{\alpha}$. The modified value of α changes the ratio of

$\dfrac{a}{\alpha} = \dfrac{(w1 - b)(1 + w_2\beta / \alpha)}{(1 - w_1 c / a)(w_2 - \gamma)}$ to $\begin{pmatrix} a \\ \alpha \end{pmatrix}_{\mathrm{m}} = \dfrac{(\Gamma_\ell + \varepsilon)(w1 - b)(1 + w_2\beta / \alpha)}{(\Gamma_\ell)(1 - w_1 c / a)(w_2 - \gamma)}$. Thus the ratio of $\dfrac{a}{\alpha}$ that was independent of the reflection standard is modified to $\begin{pmatrix} a \\ \alpha \end{pmatrix}_{\mathrm{m}}$ that is now dependent on the reflection standard value as well. The next step in the TRL de-embedding makes use of the ratio of $\dfrac{a}{\alpha}$ and the product of a and α obtained from Equation (A.32) to eliminate the α term and obtain the equation for a. The equation

to determine the value of a obtained from the original TRL de-embedding algorithm is modified due to the changed equation of $\begin{pmatrix} a \\ \alpha \end{pmatrix}_{\mathrm{m}}$ to include the reflection standard value. Hence the equation for a changes from

$a = \pm\sqrt{[(w_1 - b)(1 + w_2\beta/\alpha)(d - bf)]/[(w_2 + \gamma c/a)(1 - ec/a)]}$ obtained from the original TRL de-embedding algorithm to

$a = \pm\sqrt{[(1 + \varepsilon/\Gamma_\ell)(w_1 - b)(1 + w_2\beta/\alpha)(d - bf)]/[(w_2 + \gamma c/a)(1 - ec/a)]}$

If the reflection standard value seen at port 1 and 2 is not exactly the same, then the proof above predicts that the term for a will be dependent on the value of the reflection standard as well as on the value of ε which denotes the variation in the reflection standard value seen at the two ports.

From the above derivation it is seen that the value of a varies by the error factor $\sqrt{1 + \varepsilon/\Gamma_l}$. It is clearly seen that the amount of error introduced in the original TRL de-embedding algorithm is directly proportional to the value of ε which represents the amount of variation of the reflection standard value seen at port 2 from the reflection standard value seen at port 1. The error factor is also inversely proportional to the value of the selected reflection standard. The smaller the value of the selected reflection standard, the greater will be the error introduced in predicting the correct value of a. In order to minimize the error factor, it is easily observed that the reflection standard with magnitude of 1 will result in least variation of the predicted value of a. Hence to improve accuracy the reflection standard should be chosen to be either a short or an open.

The accuracy in the measurement of a is very important because the TRL de-embedding algorithm makes use of the value of a to determine the other parameters

of the fixture error matrices. Any discrepancies will lead to an inaccurate prediction of the fixture error matrices that will subsequently lead to an inaccurate calculation of the S parameters of the device under test. In the next paragraph analysis is done to show how the error factor of $\sqrt{1+\varepsilon/\Gamma_l}$ introduced in the value of a affects the values of the other fixture error matrix parameters.

The TRL algorithm makes use of the value of a to calculate other parameters of the error matrices. With reference to Appendix A, after obtaining the value of a, the equation of $\frac{a}{\alpha} = \frac{(w1-b)(1+w_2\beta/\alpha)}{(1-w_1c/a)(w_2-\gamma)}$ is used to calculate the value of α. Taking the error factor into consideration, the new corrected value of a denoted by a_m is given by $a_m = a(\sqrt{1+\varepsilon/\Gamma_l})$. This variation in the measured value of a causes the value of α to be modified to $\alpha_m = \frac{\alpha}{\sqrt{1+\varepsilon/\Gamma_\ell}}$. After finding the value of α, the equation for $\frac{\beta}{\alpha}$, Equation (A.31), obtained during the TRL de-embedding procedure is used to calculate the value of β. Taking into consideration the error factor that modified the value of α to $\alpha_m = \frac{\alpha}{\sqrt{1+\varepsilon/\Gamma_\ell}}$, the corrected value of β denoted by β_m is given by

$$\beta_m = \frac{\beta}{\sqrt{1+\varepsilon/\Gamma_\ell}}.$$

Finally Equation (A.23) that is the ratio of $\frac{a}{c}$ is used to calculate the value of c. Taking into consideration the error factor that modifies the value of a, the corrected value of c denoted by c_m is given by $c_m = c(\sqrt{1+\varepsilon/\Gamma_l})$. The remaining parameters of the error matrices namely b and γ do not require the value of a and hence are not

affected by the error factor that modifies the value of a. The analysis presented here shows how an incorrect prediction of the error parameter a can lead to further inaccuracies in determining other parameters of the error matrices and ultimately leading to inaccuracies in determining the S parameters of the device under test.

In the above sections a new source of possible error in the TRL calibration procedure is introduced and studied in detail. The following sections present an explanation that delve into the reason for the absence of the errors introduced due to arbitrary reflection coefficient in a new calibration technique, the Through Line (TL) calibration that under certain conditions is a replacement to the TRL calibration procedure. Another phenomenon, the discrepancies in the measurements when the difference between the through and the line standard approaches integer multiple of a quarter wavelength, observed in the TRL calibration as well as in the TL calibration technique is investigated.

4.2 Comparisons between TRL and TL Calibrations

The Through Line (TL) calibration is a two tier calibration procedure. The first step in TL calibration is to do OSL calibration followed by two set of measurements using the through and the line standards. The TL calibration, as compared to the TRL calibration procedure, needs a reduced number of standards for measurements and requires fewer connections to the microstrip ports improving the repeatability of this connection. The most important difference between the TRL and the TL calibration is that in TL calibration the reflection coefficients are derived mathematically (as shown in chapter 2), which makes it possible to "insert" ideal open and short circuits within a non-insertable medium such as a dielectric loaded waveguide. Since the value of the

reflection standard is mathematically derived, its value is determined accurately as compared to the TRL calibration procedure where it is seen that a slight variation in the reflection standard seen at the two ports causes inaccuracies in the measurements. Another inherent assumption in the TL calibration is that the fixtures are assumed to be symmetric, as compared to the TRL calibration where the fixtures are assumed to be non symmetric. As was seen in Chapter 2, symmetric fixturing simplifies the signal flow graph and makes de-embedding possible with only two set of measurements. In contrast TRL calibration requires three set of standards. The use of only two standards in TL calibration as compared to the three standards used in TRL calibration also reduces discrepancies caused in measurements due to repeatability and connectivity errors. The TL procedure determines the frequency dependent characteristic impedance of the line standard. The characteristic impedance of the line standard is determined from the scattering parameter measurements and the measured free space capacitance of the reference line.

One inherent drawback present in both the TRL and TL calibration procedure is the discrepancies in the measurements when the line difference between the through and the line standard approaches a quarter of a wavelength. The following section presents analysis that accounts for this cause of discrepancies present in the TRL and TL calibration technique. Mondal and Chen [2] have presented mathematical analyses that discuss the cause of discrepancies in the TRL calibration procedure. In the following section an alternative mathematical analysis is presented to explain why these discrepancies are likely to be present in any calibration procedure that employs delay and through as the two standards for calibration.

From the TRL calibration procedure the propagation constant is determined to be

$$e\ \exp[2\gamma(\ell_2-\ell_1)]=\frac{t_{11}+t_{22}\pm R}{t_{11}+t_{22}\mp R}\ \text{where}\ R=\sqrt{[(t_{11}-t_{22})\exp 2+4t_{12}t_{21}]}$$

In the above equation the elements t_{11}, t_{12}, t_{21} and t_{22} represent the T parameters of the measurement taken in TRL calibration. This matrix is the product of the line standard measurement of length ℓ_2 and the inverse matrix of the through standard measurement of length ℓ_1 (typically zero). This matrix can be referred to Equation (A.9) in Appendix A. Assuming that the measured S parameters, S_{11} and S_{22} (for both line and through standard measurements) are 0, the T parameters t_{12} and t_{21} (for both line and through standard measurements) become 0 as well. Hence the propagation constant becomes a function of the t_{11} parameters of lines ℓ_1 and ℓ_2 (denoted by $t_{11\ell1}$ and $t_{11\ell2}$) and t_{22} parameter of line ℓ_1 and ℓ_2 (represented by $t_{22\ell1}$ and $t_{22\ell2}$). This can be presented in the matrix form as

$$\begin{bmatrix} t_{11} & t_{12} \\ t_{21} & t_{22} \end{bmatrix} = \begin{bmatrix} t_{11\ell1} & 0 \\ 0 & t_{22\ell1} \end{bmatrix} \begin{bmatrix} t_{11\ell2} & 0 \\ 0 & t_{22\ell2} \end{bmatrix}^{-1}$$

where $t_{11} = t_{11\ell1} / t_{11\ell2}$ and $t_{22} = t_{22\ell1}/t_{22\ell2}$.

The above assumption also modifies the propagation constant equation to

$$e\ \exp[2\gamma(\ell_2-\ell_1)]=\frac{t_{11}+t_{22}\pm(t_{11}-t_{22})}{t_{11}+t_{22}\mp(t_{11}-t_{11})}\ \text{or}\ e\ \exp[2\gamma(\ell_2-\ell_1)]=\frac{t_{11}}{t_{22}}or\frac{t_{22}}{t_{11}}.$$

Substituting $t_{11} = t_{11\ell1} / t_{11\ell2}$ and $t_{22} = t_{22\ell1}/t_{22\ell2}$ in the above equations for propagation constant yields

$$e\ \exp[2\gamma(\ell_2-\ell_1)]=\frac{t_{11\ell1}t_{22\ell2}}{t_{22\ell1}t_{11\ell2}}=\frac{t_{22\ell1}t_{11\ell2}}{t_{22\ell2}t_{11\ell1}}.$$

Converting the T parameters to S parameters yields

$$e\ \exp[2\gamma(\ell_2-\ell_1)]=\frac{S_{12\ell1}S_{21\ell1}}{S_{12\ell2}S_{21\ell2}}=\frac{S_{12\ell2}S_{21\ell2}}{S_{12\ell1}S_{21\ell1}}.$$

The following assumption is made that $S_{12} = S_{21}$. With this assumption the above equations further simplify to $e \exp[\gamma(\ell_2 - \ell_1)] = \frac{S_{12\ell 1}}{S_{12\ell 2}} = \frac{S_{12\ell 2}}{S_{12\ell 1}}$.

As seen from the above simplified equations, the propagation constant is directly proportional to the S_{12} measurements of the line and through standards.

After deriving the equation for the propagation constant, further analysis is done in the following paragraphs to show the cause of discrepancies in the measurements when the difference between the delay standards approach an integer multiple of a half wavelength.

The propagation constant derived for the line standard can be represented in magnitude and phase notation or as $p = \frac{|S_{12\ell 1}|}{|S_{12\ell 2}|} * e \exp[j(\angle S_{12\ell 1} - \angle S_{12\ell 2})]$. The magnitude phase notation can also be represented in complex number notation as

$p = R + jI$ where $R = \frac{|S_{12\ell 1}|}{|S_{12\ell 2}|} \cos(\angle S_{12\ell 1} - \angle S_{12\ell 2})$ and

$I = \frac{|S_{12\ell 1}|}{|S_{12\ell 2}|} \sin(\angle S_{12\ell 1} - \angle S_{12\ell 2})$.

From the real and imaginary terms of the propagation constant equation, it is seen that the determination of the propagation constant is dependent on the insertion phase of the delay standard. The insertion phase of a line is directly proportional to the frequency and the line length and inversely proportional to the wavelength. Hence the selection of the line length, which is the difference between the line lengths of the two delay standards, the through and the line standard in TRL and TL calibration, decides the insertion phase. When the line difference approaches a quarter of a wavelength, the insertion phase approaches 90º.

We now analyze the effect of variation in the insertion phase (which is decided by the difference of the line standards) on the real and imaginary parts of the propagation constant equation. When the standard lengths ℓ_1 and ℓ_2 are chosen in the range of $0 < (\ell_1 - \ell_2) < \frac{\lambda}{4}$, both the real and imaginary parts of p are positive. In other word the insertion phase is between 0º and 90º, hence both the cosine term in the real part and the sine term in the imaginary part remain positive. For the line difference in the range of $\frac{\lambda}{4} < (\ell_1 - \ell_2) < \frac{\lambda}{2}$, the real part is negative and the imaginary part is positive. Hence the arguments of p are used to keep track of the correct angular rotation for the expression of the propagation constant. Another observation is that when the line difference approaches 0º or 180º, the real part of p that represents the attenuation constant becomes very high (the cosine of 0º and 180º becomes ± 1) and the imaginary part that represents the propagation constant becomes very small and approaches zero. The large variations in the real and imaginary part of p caused when the insertion phase approaches 0º or 180º is the main cause of the observed discrepancies in the TRL and TL calibration procedure. Also the selection of the line difference in the range of $\frac{\lambda}{4}$ is justified because at this length the insertion phase approaches 90º which causes the real part to be very small thereby reducing errors in the attenuation constant determination.

4.3 Conclusion

This chapter discussed in details a new source of error inherent in the TRL calibration. The proposed source of error is based on the assumption that the

reflection standard value seen at the two ports of the network analyzer are not exactly same. The TRL calibration method is compared with the new calibration method, the TL calibration to explain why this calibration, under certain conditions is a better alternative to TRL calibration. The proposed source of error present in TRL calibration is avoided in TL calibration because it makes use of symmetry fixtures and synthesized reflection co-efficient that simplifies the error model and reduces the number of standards needed thereby reducing the repeatability error. Another drawback of TRL namely the accurate determination of the characteristic impedance is removed in TL calibration by determining the impedance of the line from the scattering parameters measurements and the measured free space capacitance of the line. Finally the cause of discrepancies in the TRL and TL calibration measurement when the difference in the length of the through and line standard approaches 0 or $\frac{\lambda}{2}$ is discussed.

Chapter 5: Experimental Results

The proposed discrepancies introduced in the parameters of the error boxes A and B due to the arbitrary reflection coefficient are verified experimentally. The proposed error model is based on the assumption that the reflection standard value seen at the two ports are not exactly same. In the experimental setup, this assumption is verified experimentally. Experimental analysis is done using symmetric fixture on the device under test and the readings are processed with the TRL algorithm implemented in MATLAB to obtain the parameters of the error box A and B. Next the error factor term introduced due to mismatch in the reflection coefficient is introduced into the MATLAB implementation of the TRL algorithm and the new set of parameters for the error box A and B are obtained. The above process is repeated for different reflection coefficient standards to obtain an optimal value of reflection standard that result in least error. The results are verified and presented in this chapter.

5.1 General Measurement Steps

The network analyzer measurement system consists of the source, the test set, the vector signal processor and the display. These together comprise the stimulus and response test system that measures the signal transmitted through the device and the reflected signal from the input of the device. The data is then processed to display the magnitude and phase responses. For our measurements a Hewlett Packard 8510 network analyzer system is used. This network analyzer contains a sweeper to provide the RF stimulus. The test set provides the points where the device under test is to be connected. The system uses coaxial test sets up to frequency range of 50 GHz. The front panel of network analyzer includes the CRT that displays the measurement

results. The network analyzer has two channels for displaying the measurements at the two test ports. ‘Channel 1’ or ‘Channel 2’ selects the channel display. The keys in the ‘Stimulus’, ‘Parameter’, ‘Format’ and ‘Response’ blocks are needed for the measurement setup, calibration, data representation and data output functions. Following are the general measurement sequence involved while taking measurements. The first step is to setup the test port cables and select suitable connectors for the device under test. The next step is to setup the network analyzer, which involves using the keys in the ‘Stimulus’ block to set the desired start and stop frequencies, number of measured points and characteristic of frequency sweep. The keys in the ‘Parameter’ block decide the parameters to be measured and displayed. The keys in the ‘Format’ and ‘Response’ blocks are used for selecting type of display and position of the trace to view the measured data respectively. Next step is to select the appropriate calibration standard to correct the systematic errors using the keys in the ‘Cal’ block. Once the measurements have been taken, the ‘save’ key stores the measured data in internal/external storage. The ‘Marker’ key and knob is used to position the measurement markers to the points of interest on the trace and store these results without further recalibration. The above-mentioned steps give a brief outline to take basic measurements in network analyzer and introduce the reader to the network analyzer control keys.

5.2 Experiment Setup

After an overview of the basic control keys and measurement sequence, we discuss in detail the fixtures used for our measurement setup, the components used and the procedure employed in getting the corrected measured S parameters of the device under test.

Before starting with the measurements the network analyzer need to be configured by the user to display the measurements accordingly. The front panel keys mentioned in the above section can easily configure the network analyzer. The following steps mentioned here provide an overview of the configuration settings used by us in taking the measurements. The keys in the 'Stimulus' block are used to set the frequency sweep, the sweep time and the number of frequency points to be measured to 801 points. The 'start' and 'stop' keys and the 'center' and 'span' keys on the 'Stimulus' block are used to set the limits of the frequency sweep. Pressing the 'Stimulus' menu key gives options to set the sweep time, number of points and sweep modes. To select the number of points, press the 'Number of points' softkey to select the 801 points. The 'Ramp', 'Step' and 'Frequency List' softkeys select the sweep mode. The keys in the 'Parameter' block allow the user to select the S parameters to be measured. In our experiment all the S parameters were measured and stored. The next step after configuring the network analyzer for measurements is to perform the measurement calibration. The keys on the 'Format' block provide a comprehensive selection of keys to display the measurements in different display formats. The calibration kit used is a Hewlett Packard 85050 7 millimeters Calibration Kit. The calibration standard definitions for the above mentioned Calibration Kit are stored in the internal memory of the network analyzer prior to starting the measurements. The standard definitions provide the constants needed to mathematically model the electrical characteristics of the standards used in the Calibration Kit.

The point where the device under test is connected is called the 'Reference Plane', which is the end of the coaxial cable. In our case the test set consists of the coaxial cables and fixtures that connect the network analyzer and the coaxial cable.

Calibration is necessary before taking measurements as the interconnecting of the test set coaxial cables influences the accuracy of the measurement. In order to remove these systematic errors the Open-Short-Load (OSL) calibration method is used to setup the reference plane to the coaxial probe tips at port 1 and 2 of the network analyzer. For better accuracy low band load is used as the 'Load' standard in OSL calibration for frequencies below 2 GHz and the sliding load is used for measurement above 2 GHz. Since the frequency range for our measurement is up to 18 GHz, sliding load standard is used in the OSL calibration. The main aim of the experiment is to obtain the parameters of the error box A and B and finally obtain the correct S parameters of the device under test by implementing the TRL algorithms and the modified TRL algorithm that takes into consideration the error factor introduced due to arbitrary reflection standard and compare their differences. In order to introduce these errors, symmetrical fixtures are introduced in between the reference plane and the device under test. The symmetrical fixtures are constructed from connecting "7mm - SMA type adapter to 90º bend SAM type to SMA – 7mm type adapter" at both ends of the test set coaxial cables. The next step after the OSL calibration is to select the Calibration kit. In our experimental setup, for maximum accuracy, the FULL 2-PORT calibration choice offered in the network analyzer HP 8510 is selected. The FULL 2-PORT calibration uses Open, Short and Load standards at each port 1 and 2 of the network analyzer. The FULL 2-PORT calibration is selected in the network analyzer from the Cal type selection menu. In the following paragraph, the different steps involved in the FULL 2-PORT calibration method implemented in our experimental setup are listed.

The first three steps involve connecting the short, open and load standards at the two ends of the connected fixtures and noting the reflection coefficient value,

yielding six sets of measurements. The next four steps involve connecting a 20 dB attenuator and open/short standards at the two reference planes, which are the ends of the connected fixtures. Similar measurements are taken by replacing the 20 dB attenuator with a 50 dB attenuator. In the next step, the 20 dB attenuator is connected between the two fixture ends. For the thru measurement, the two fixture ends are connected together. The next step involves connecting the 20 dB attenuator and a 10 cm air line between the reference planes, which are the two ends of the connected fixtures. Similar measurements are taken by replacing the 20 dB attenuator with a 50 dB attenuator. The calibration kit used for our set of measurements did not contain the 'Reflect' standard. In other words, the TRL calibration kit is not unavailable. Hence the TRL deembedding algorithm is implemented in MATLAB and the set of measurements obtained from the FULL 2-PORT CALBRATION are fed into the MATLAB code that processes the set of measurements, performs the TRL deembedding algorithm and displays the results. The following section presents the observed results for the above set of measurements taken and confirms the theoretical assumption of discrepancies in the observed reflection coefficient seen at the two ends of the reference planes, which are the two ends of the connected symmetrical fixtures.

5.3 MATLAB Simulation Results

In the following paragraphs, the measurements obtained from the experimental procedure, as mentioned in the previous section, are presented. The measured data obtained from the above mentioned steps are fed into the MATLAB code that implements the TRL deembedding algorithm. After processing the data, the reflection coefficients seen at the ports of the network analyzer are seen to be different. The proposed source of discrepancies in TRL calibration was based on the following assumption that the reflection coefficients seen at the end of the two ports of the network analyzer are different. This assumption is verified by the MATLAB code. The MATLAB code further implements the modified TRL deembedding procedure that estimates the amount of error introduced in the error boxes A and B due to the observed discrepancies in the reflection coefficient seen at the end of the ports of the network analyzer.

5.3.1 TRL calibration results obtained from using short and open standards

The experimental analysis is done is by implementing TRL algorithm on three different devices under test and then comparing their results. The first device under test is an air filled transmission line connected between the ends of the two fixtures. The second device under test used is a 20dB attenuator. The third device used is a combination of 20dB attenuator and an air filled transmission line.

Figure 5.1 shown in the next page shows the data obtained from the network analyzer in magnitude and phase response for the reflection coefficient of the short standard connected at the two symmetrical fixture ends.

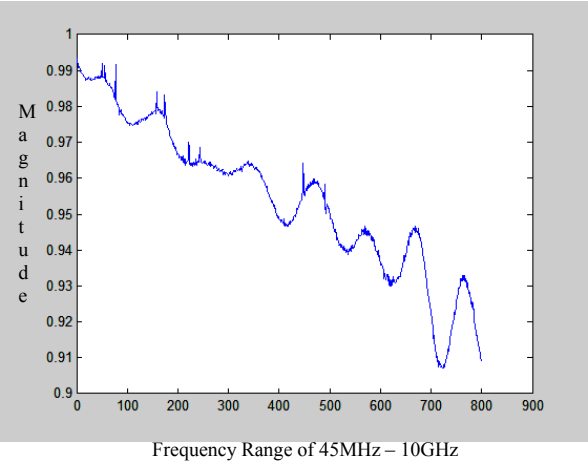

Frequency Range of 45MHz – 10GHz
Divided into 801 equal points

(a)

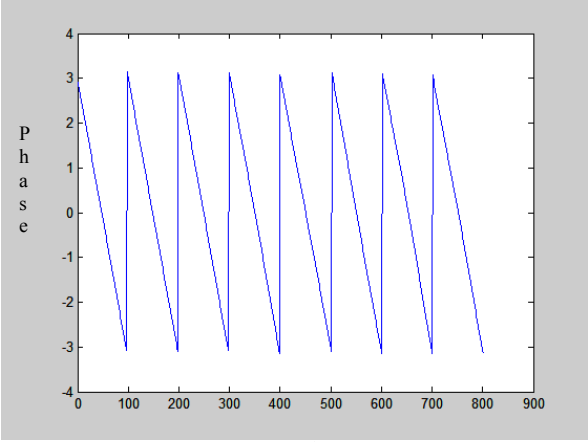

Frequency Range of 45MHz – 10GHz
Divided into 801 equal points

(b)

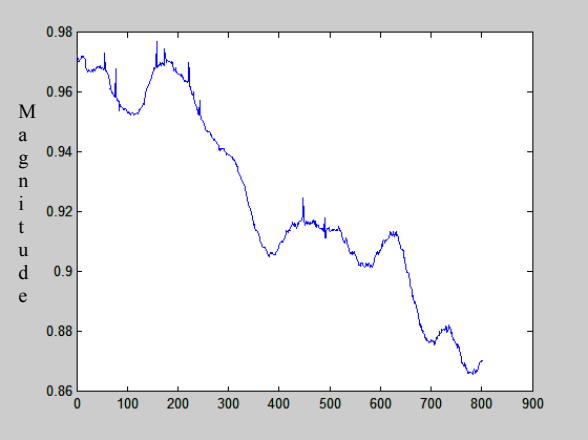

Frequency Range of 45MHz – 10GHz
Divided into 801 equal points

(c)

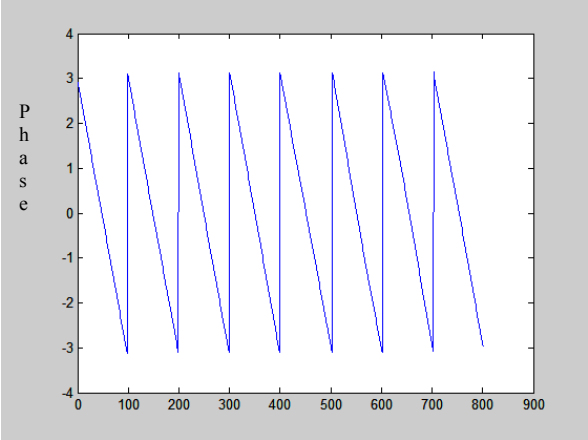

Frequency Range of 45MHz – 10GHz
Divided into 801 equal points

(d)

Figure 5.1: Reflection coefficients of the short standard: (a) magnitude at Port 1;

(b) phase at Port1; (c) magnitude at Port 2; and (d) phase at Port 2.

Similarly Figure 5.2 and Figure 5.3 below show the data obtained from the network analyzer in magnitude and phase response for the reflection coefficient of the open and match standard respectively.

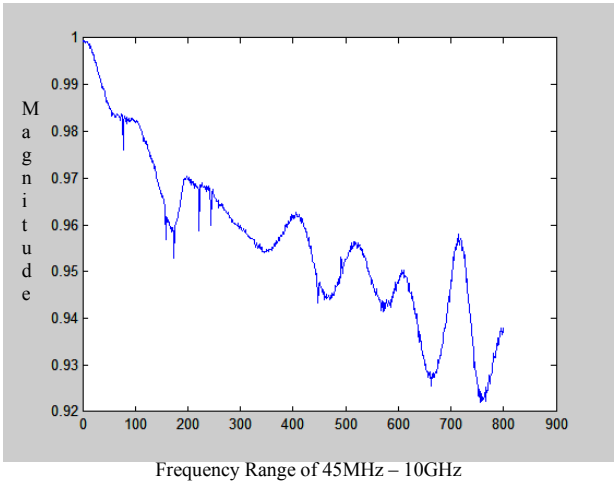

Frequency Range of 45MHz – 10GHz
Divided into 801 equal points

(a)

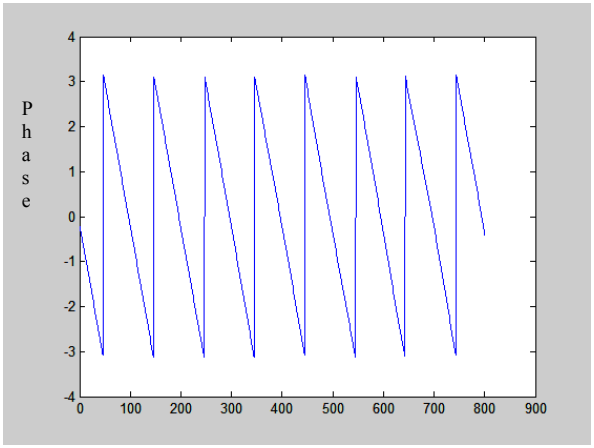

Frequency Range of 45MHz – 10GHz
Divided into 801 equal points

(b)

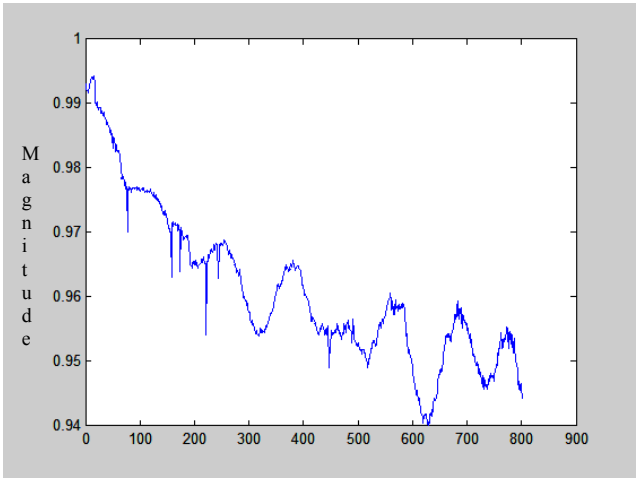

Frequency Range of 45MHz – 10GHz
Divided into 801 equal points

(c)

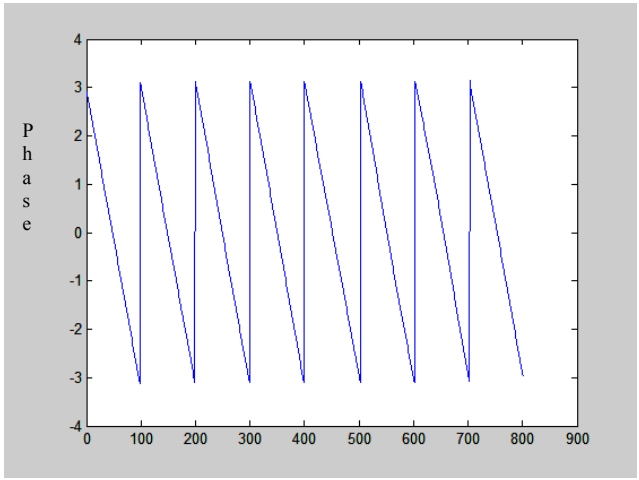

Frequency Range of 45MHz – 10GHz
Divided into 801 equal points

(d)

Figure 5.2: Reflection coefficients of the open standard: (a) magnitude at Port 1; (b) phase at Port1; (c) magnitude at Port 2; and (d) phase at Port 2.

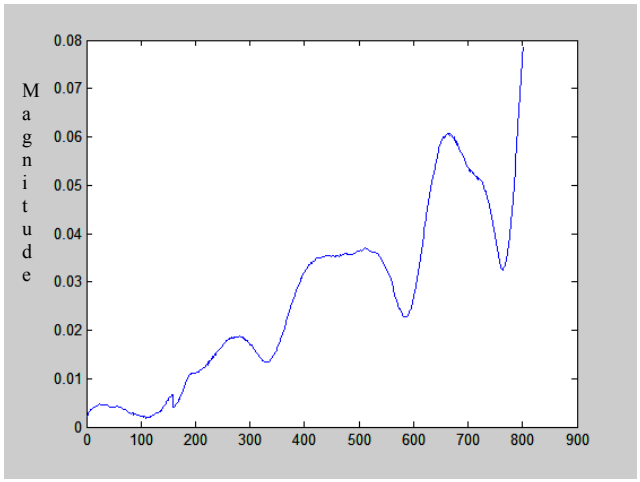

Frequency Range of 45MHz – 10GHz
Divided into 801 equal points

(a)

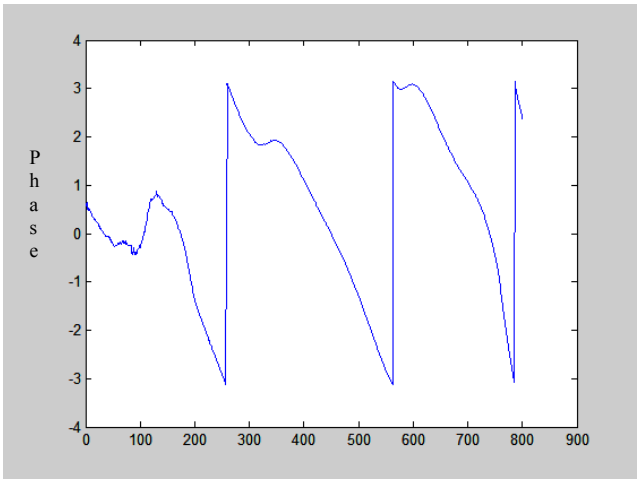

Frequency Range of 45MHz – 10GHz
Divided into 801 equal points

(b)

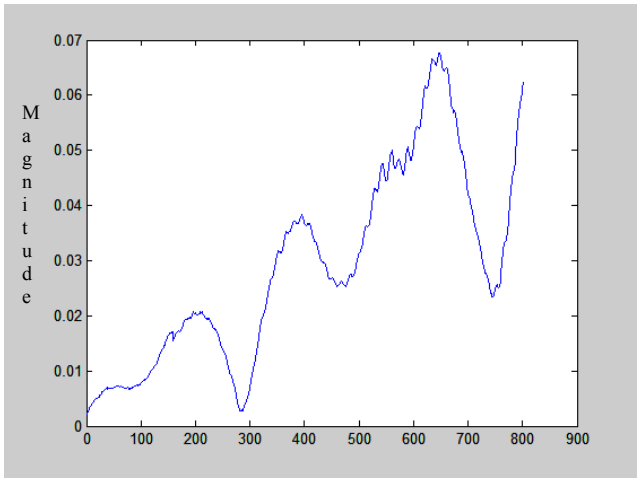

Frequency Range of 45MHz – 10GHz
Divided into 801 equal points

(c)

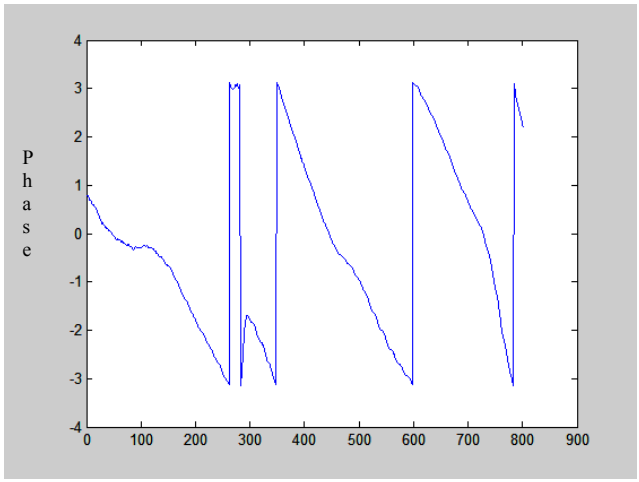

Frequency Range of 45MHz – 10GHz
Divided into 801 equal points

(d)

Figure 5.3: Reflection coefficients of the match standard: (a) magnitude at Port 1;

(b) phase at Port1; (c) magnitude at Port 2; and (d) phase at Port 2.

The following sections in the next page provide the results for the TRL calibration on the three devices under tests.

5.3.1.1 TRL Calibration for an air filled transmission line

The air filled transmission line is placed in between the two fixture ends and all the four S parameters are measured. Then the thru and airline data are fed into the MATLAB code that implements the TRL deembedding procedure. The TRL deembedding procedure is implemented for the three different standards, namely short, open and match. For each of these standards, the reflection coefficient calculated from the TRL algorithm seen at the two ports is measured. As per our assumption, it is also experimentally observed that the reflection coefficient seen at the two ports are not exactly same. This reflection coefficient seen at the two ports for the different standards are shown in Figures 5.4-5.6 below.

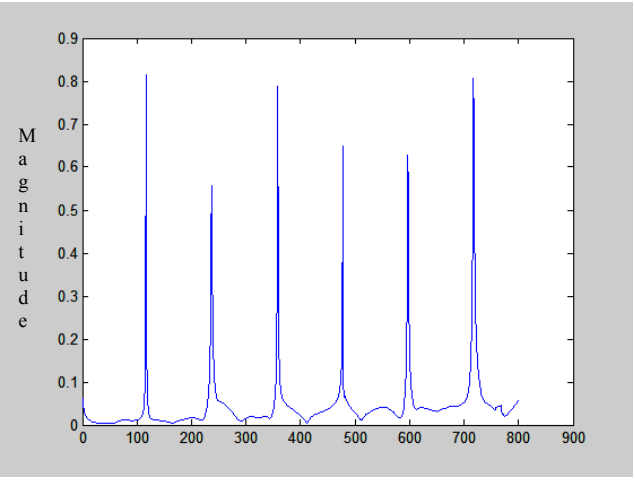

Frequency Range of 45MHz – 10GHz
Divided into 801 equal points

(a)

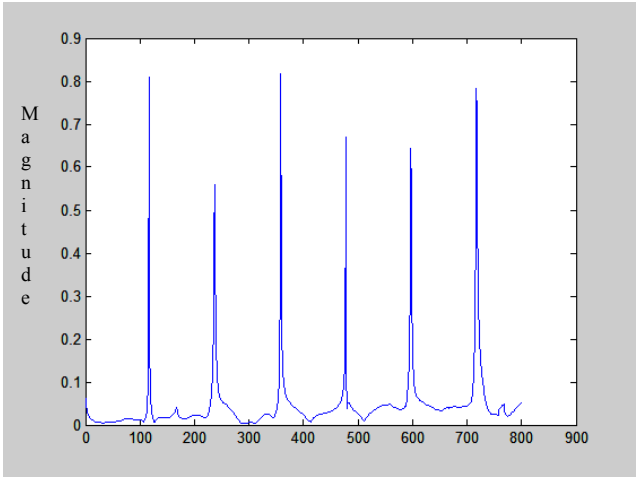

Frequency Range of 45MHz – 10GHz
Divided into 801 equal points

(b)

Figure 5.4: Calculated reflection coefficient from TRL algorithm for air filled transmission line: (a) match standard at Port 1; (b) match standard at Port 2.

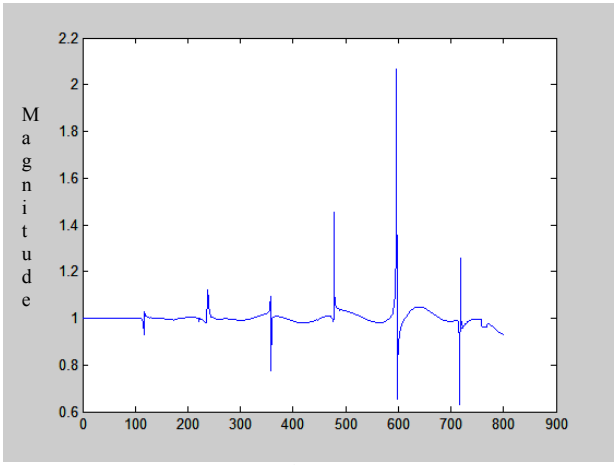

Frequency Range of 45MHz – 10GHz
Divided into 801 equal points

(a)

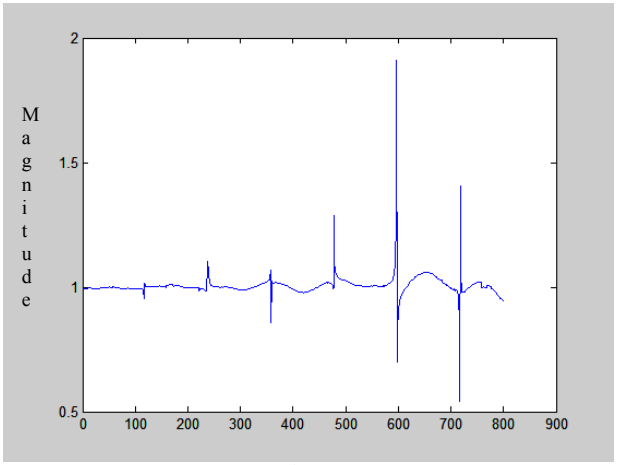

Frequency Range of 45MHz – 10GHz
Divided into 801 equal points

(b)

Figure 5.5: Calculated reflection coefficient from TRL algorithm for air filled transmission line: (a) open standard at Port 1; (b) open standard at Port 2.

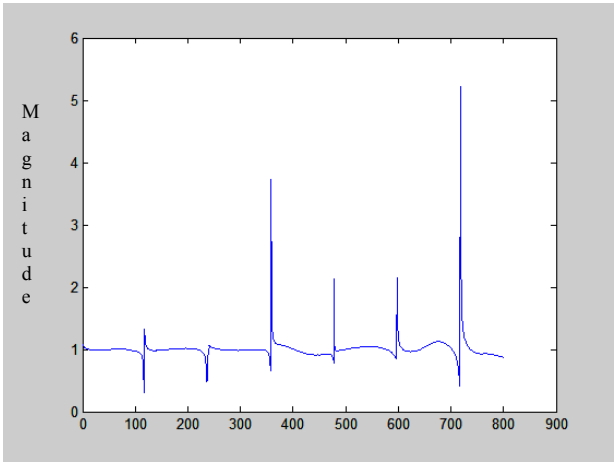

Frequency Range of 45MHz – 10GHz
Divided into 801 equal points

(e)

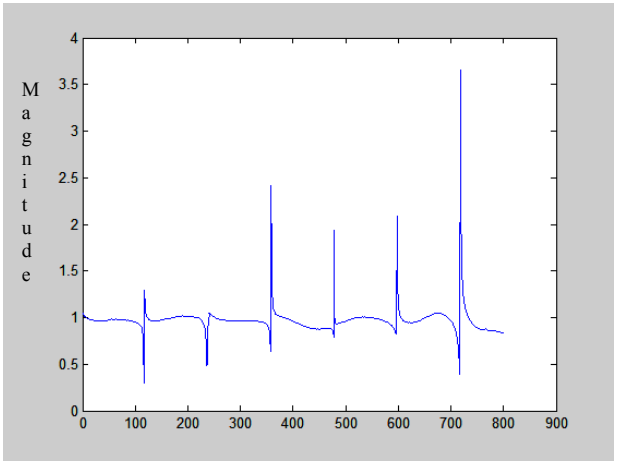

Frequency Range of 45MHz – 10GHz
Divided into 801 equal points

(f)

Figure 5.6: Calculated reflection coefficient from TRL algorithm for air filled transmission line: (a) short standard at Port 1; and (b) short standard at Port 2.

As was proposed in chapter 4, the variation in the reflection coefficient seen at the two ports of the network analyzer introduces an error factor that adds inaccuracy

to the measured value of a. Taking the error factor into consideration, the new corrected value of a denoted by am is given by $a_m = a(\sqrt{1+\varepsilon/\Gamma_l})$. As can be observed from the above error factor equation ($\sqrt{1+\varepsilon/\Gamma_l}$), the small variation in the match reflection standard seen at the two ports will cause a large variation in the error factor as compared to the short or open reflection standard. This observation is verified experimentally for the three different standards and is presented in Figure 5.7 below.

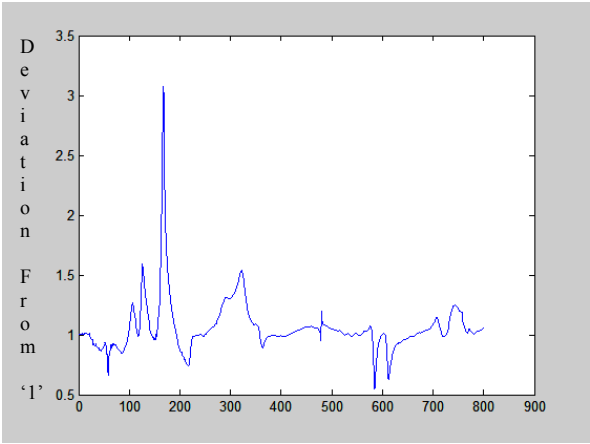

Frequency Range of 45MHz – 10GHz
Divided into 801 equal points

(a)

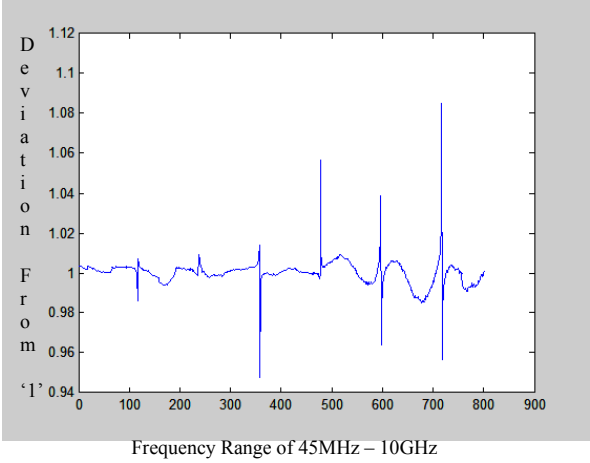

Frequency Range of 45MHz – 10GHz
Divided into 801 equal points

(b)

Figure 5.7: Error factor for different loads used in TRL procedure for air filled transmission line with: (a) match standard; (b) open standard.

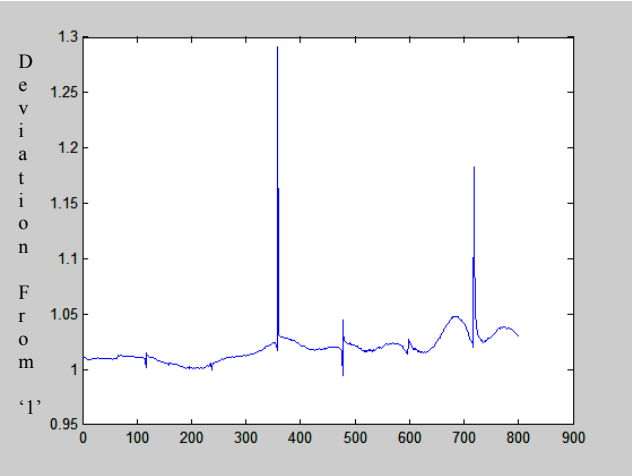

(c)

Figure 5.7: Error factor for different loads used in TRL procedure for air filled transmission line with: (c) short standard.

Thus as seen in Figure 5.7, minimum error is introduced when either open or short reflection standards are used as compared to match reflection standard.

5.3.1.2 TRL Calibration for a 20 dB attenuator

In the next step, the entire procedure mentioned above is repeated with the air filled transmission line replaced by a 20dB attenuator between the two fixtures. As per our assumption, it is again experimentally observed that the reflection coefficient seen at the two ports are not exactly same. The reflection coefficients measured from the TRL deembedding algorithm, seen at the two ports for the different standards are shown in the next pages in Figures 5.8-5.10.

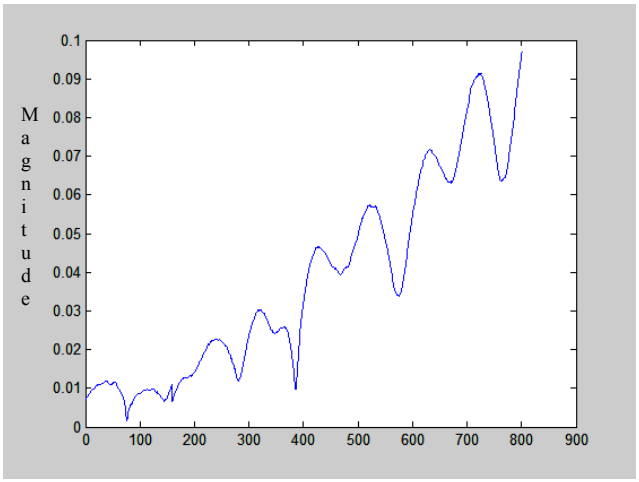

Frequency Range of 45MHz – 10GHz
Divided into 801 equal points

(a)

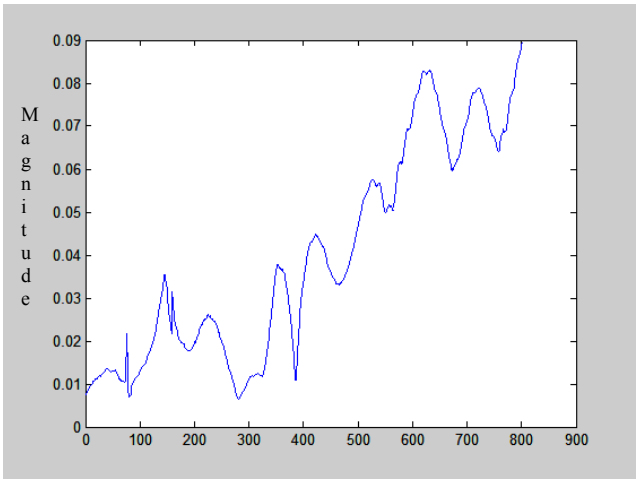

Frequency Range of 45MHz – 10GHz
Divided into 801 equal points

(b)

Figure 5.8: Calculated reflection coefficient from TRL algorithm for 20 dB attenuator:

(a) match standard at Port 1; (b) match standard at Port 2.

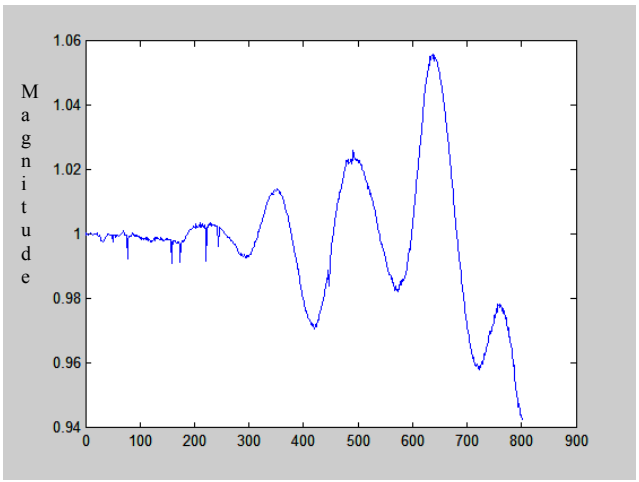

Frequency Range of 45MHz – 10GHz
Divided into 801 equal points

(a)

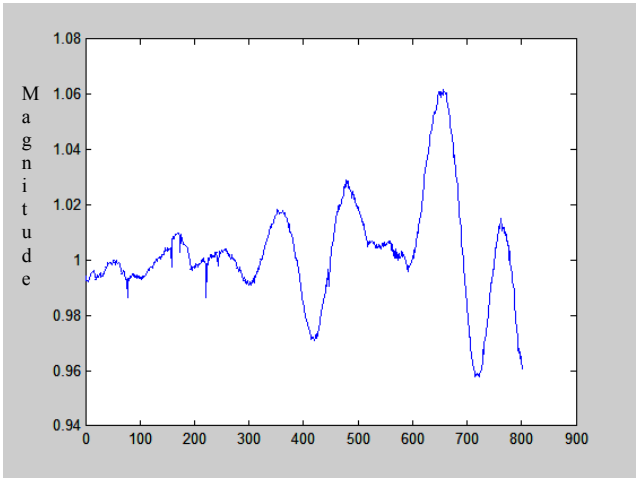

Frequency Range of 45MHz – 10GHz
Divided into 801 equal points

(b)

Figure 5.9: Calculated reflection coefficient from TRL algorithm for 20 dB attenuator:

(a) open standard at Port 1; (b) open standard at Port 2.

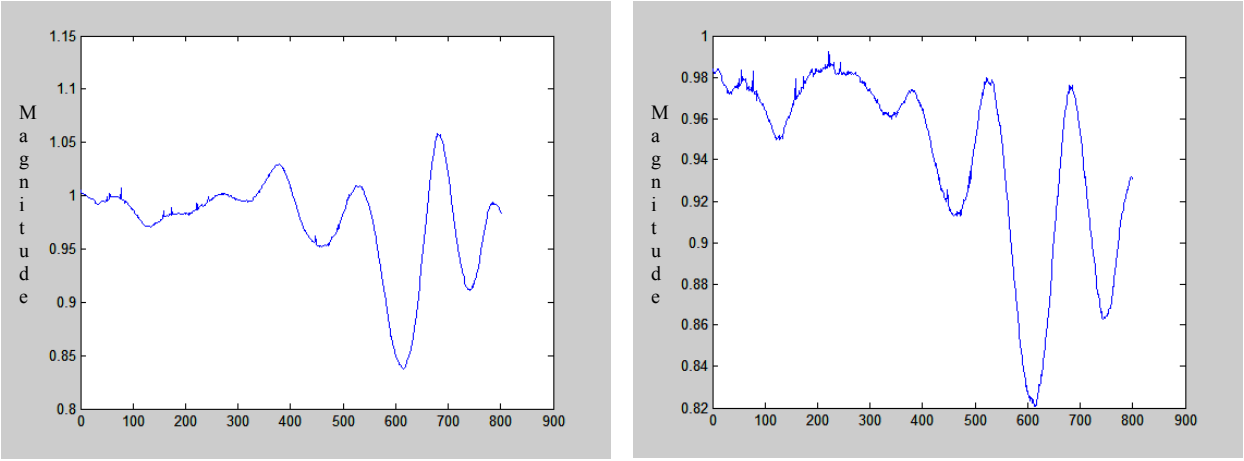

Figure 5.10: Calculated reflection coefficient from TRL algorithm for 20 dB attenuator: (a) short standard at Port 1; and (f) short standard at Port 2.

Taking the error factor into consideration, as seen before, the small variation in the match reflection standard seen at the two ports will cause a large variation in the error factor as compared to the short or open reflection standard. This observation is verified experimentally for the three different standards and is presented in Figure 5.11 in the next page.

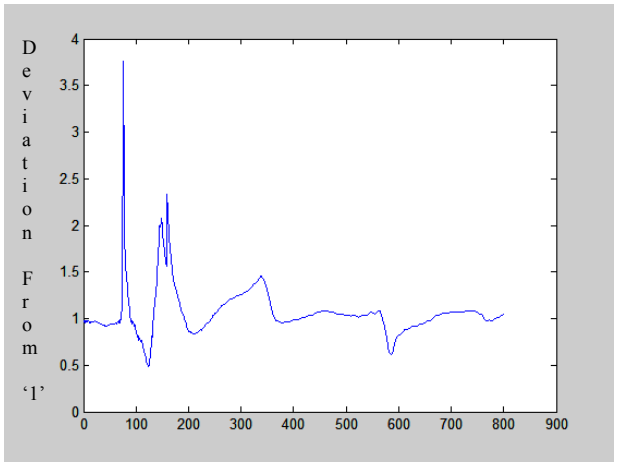

Frequency Range of 45MHz – 10GHz
Divided into 801 equal points

(a)

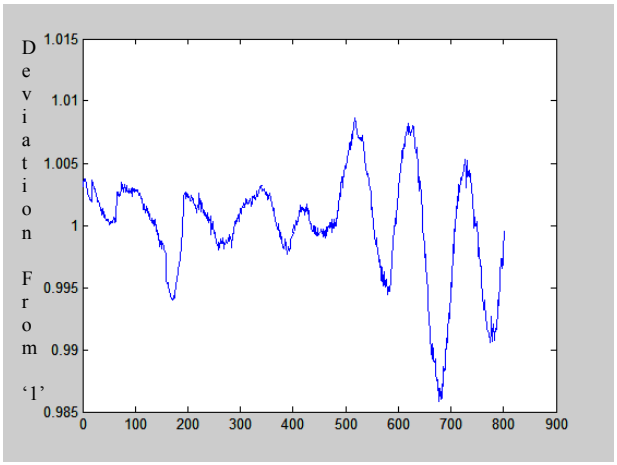

Frequency Range of 45MHz – 10GHz
Divided into 801 equal points

(b)

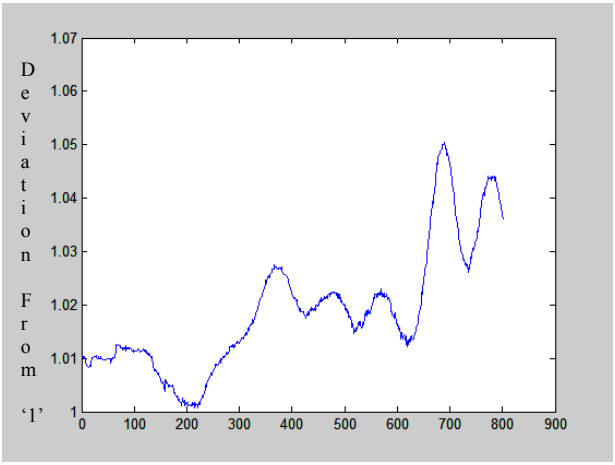

Frequency Range of 45MHz – 10GHz
Divided into 801 equal points

(c)

Figure 5.11: Error factor for different loads used in TRL procedure for 20 dB attenuator with: (a) match standard; (b) open standard; (c) short standard.

5.3.1.3 TRL Calibration for combination of 20 dB attenuator and transmission line

The entire procedure mentioned above is again repeated with the 20dB attenuator and air filled transmission line connected between the two fixtures. As per our assumption, it is also experimentally observed that the reflection coefficient seen at the two ports are not exactly same. The reflection coefficients measured from the TRL deembedding algorithm, seen at the two ports for the different standards are shown in Figures 5.12-5.14 below.

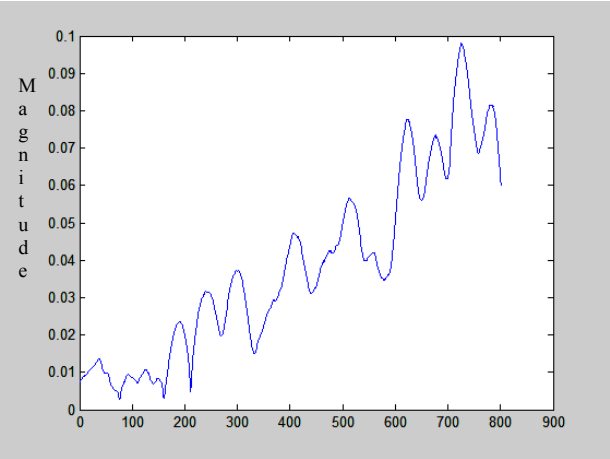

(a)

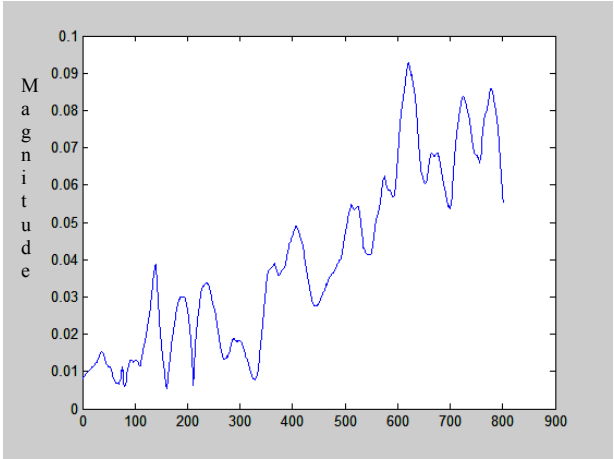

(b)

Figure 5.12: Calculated reflection coefficient from TRL algorithm for 20dB attenuator and air filled transmission line for: (a) match standard at Port 1; (b) match standard at Port 2.

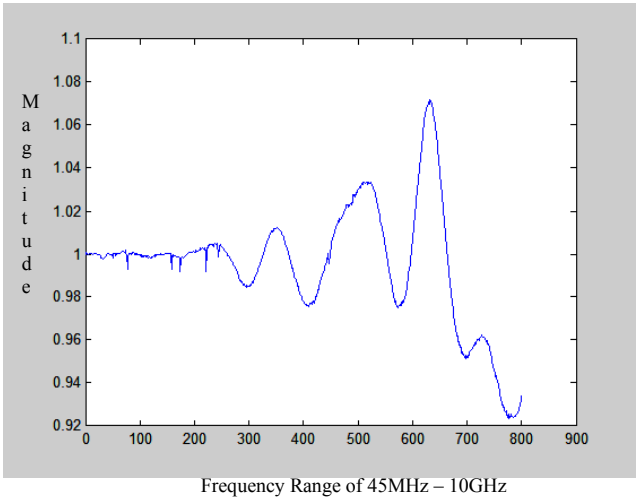

Frequency Range of 45MHz – 10GHz
Divided into 801 equal points

(a)

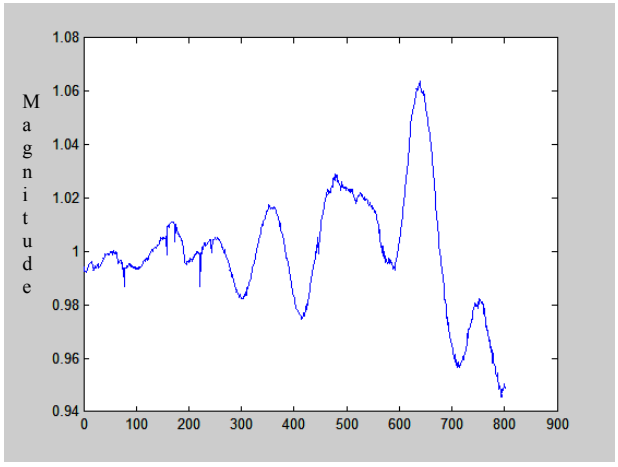

Frequency Range of 45MHz – 10GHz
Divided into 801 equal points

(b)

Figure 5.13: Calculated reflection coefficient from TRL algorithm for 20dB attenuator and air filled transmission line for: (a) open standard at Port 1; (b) open standard at Port 2.

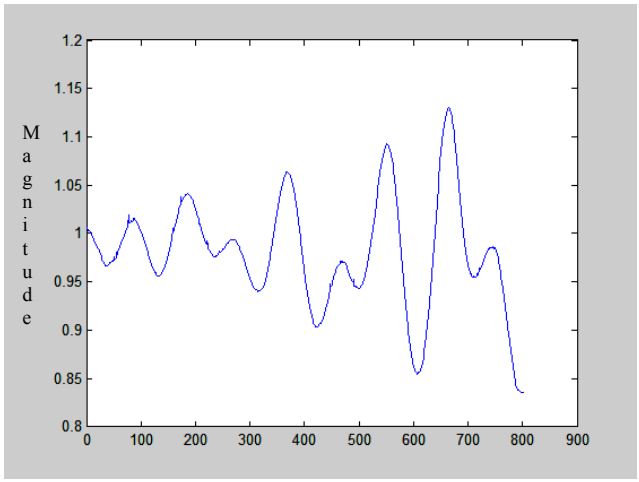

Frequency Range of 45MHz – 10GHz
Divided into 801 equal points

(a)

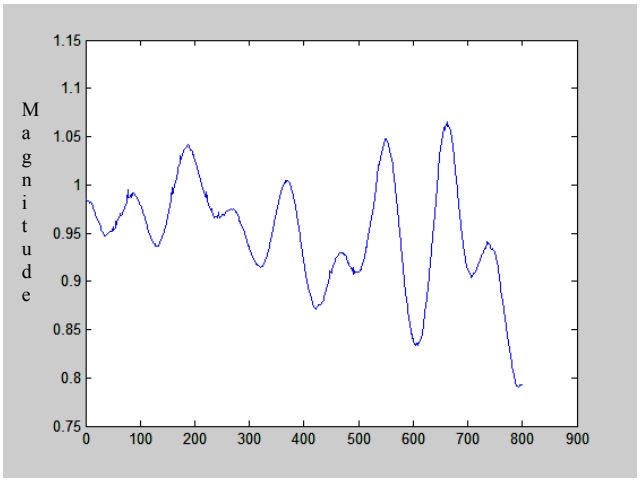

Frequency Range of 45MHz – 10GHz
Divided into 801 equal points

(b)

Figure 5.14: Calculated reflection coefficient from TRL algorithm for 20dB attenuator and air filled transmission line for: (a) short standard at Port 1; (b) short standard at Port 2.

Taking the error factor into consideration, the small variation in the match reflection standard seen at the two ports will cause a large variation in the error factor as compared to the short or open reflection standard. This observation is verified experimentally for the three different standards and is presented in Figure 5.15 below.

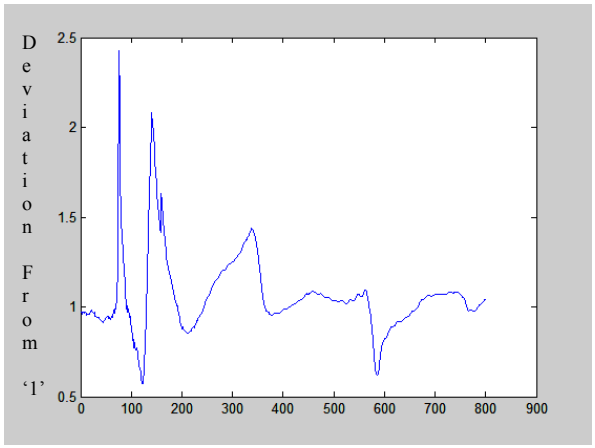

Frequency Range of 45MHz – 10GHz
Divided into 801 equal points

(a)

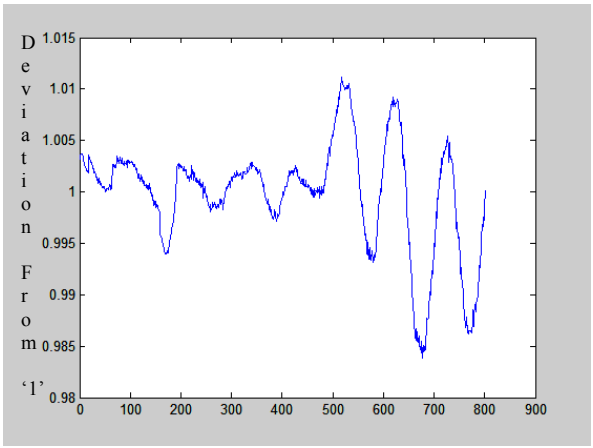

Frequency Range of 45MHz – 10GHz
Divided into 801 equal points

(b)

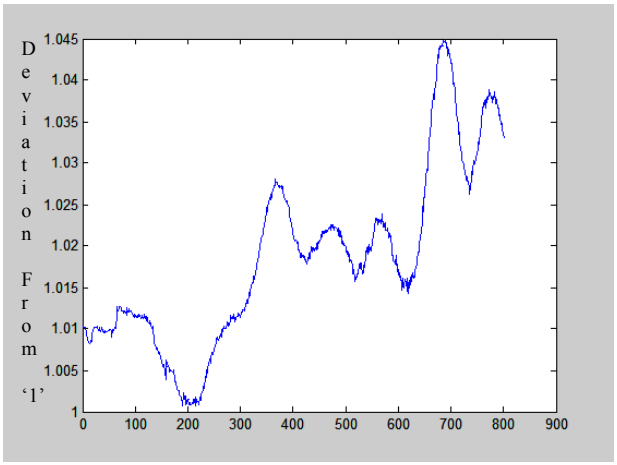

Frequency Range of 45MHz – 10GHz
Divided into 801 equal points

(c)

Figure 5.15: Error factor for different standards used in TRL procedure for the 20dB attenuator and air filled transmission line with: (a) match standard; (b) open standard; (c) short standard.

5.3.1.4 Comparison of results from TRL Calibration for the three devices

As seen from the experimental results, the error factor introduced in the TRL calibration for an air filled transmission line (as seen from Figure 5.7), for a 20dB attenuator (as seen from Figure 5.11) and for the combination of 20db attenuator and airline (as seen from Figure 5.15) show similar results, that is the error factor in all the three cases show minimum variation for short and open reflection standard and maximum variation for match standard.

5.3.2 TRL calibration results obtained from using 20dB attenuator along with short and open standards

For the next set of measurements, the open load connected at the two fixture ends are removed and instead replaced by a 20dB attenuator and an open load together. The observed reflection coefficient measurements for these new combinations are shown in Figure 5.16 below.

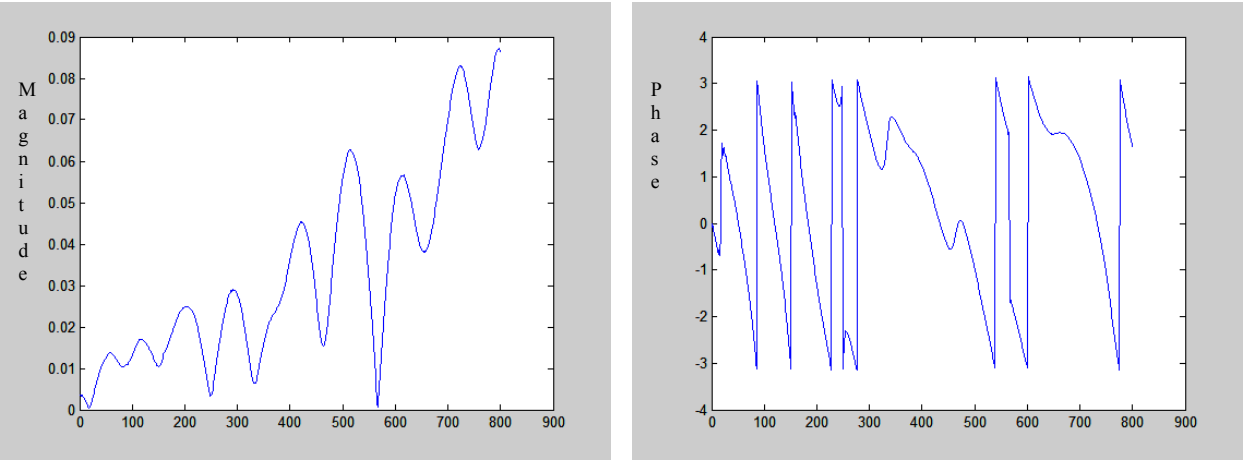

Frequency Range of 45MHz – 10GHz
Divided into 801 equal points

(a)

Frequency Range of 45MHz – 10GHz
Divided into 801 equal points

(b)

Figure 5.16: Reflection coefficients of the 20 dB attenuator and open standard:

(a) magnitude at Port 1; (b) phase at Port1.

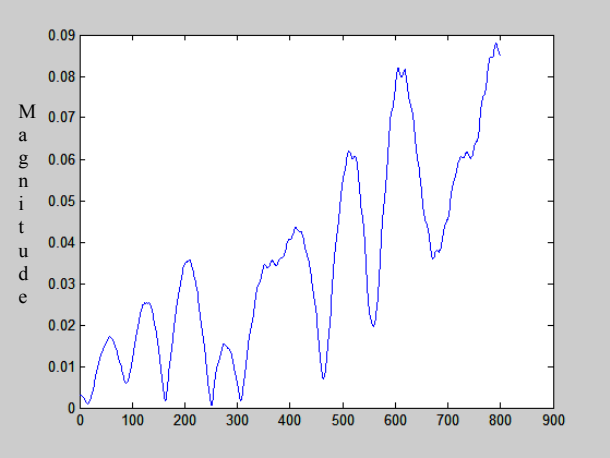

Frequency Range of 45MHz – 10GHz
Divided into 801 equal points

(c)

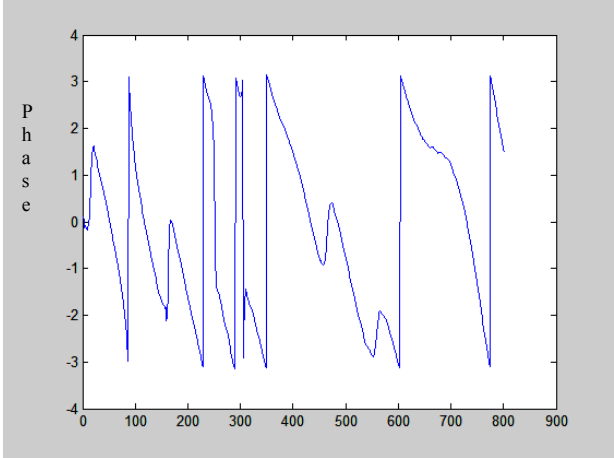

Frequency Range of 45MHz – 10GHz
Divided into 801 equal points

(d)

Figure 5.16: Reflection coefficients of the 20 dB attenuator and open standard:

(c) magnitude at Port 2; (d) phase at Port2.

Similarly, a 20dB attenuator and an open standard replace the short standard. The observed reflection coefficient measurements for these new combinations are shown in Figure 5.17 below.

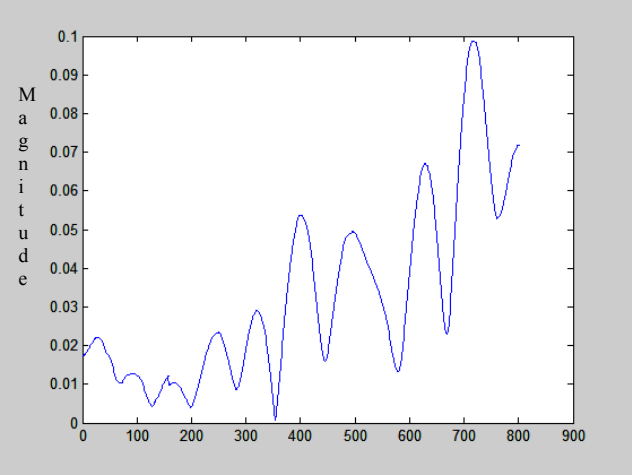

Frequency Range of 45MHz – 10GHz
Divided into 801 equal points

(a)

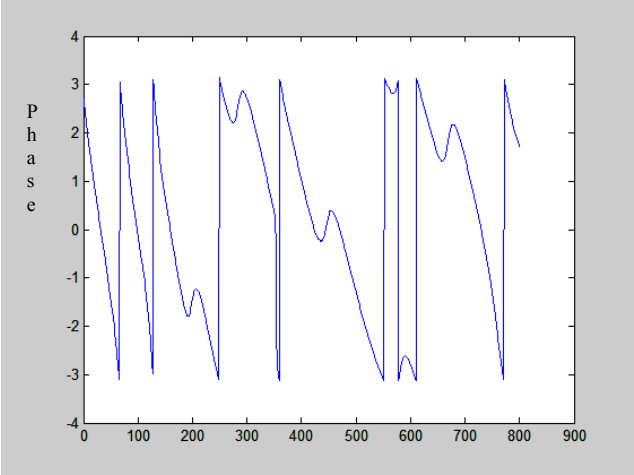

Frequency Range of 45MHz – 10GHz
Divided into 801 equal points

(b)

Figure 5.17: Reflection coefficients of the 20 dB attenuator and short standard:

(a) magnitude at Port 1; (b) phase at Port1.

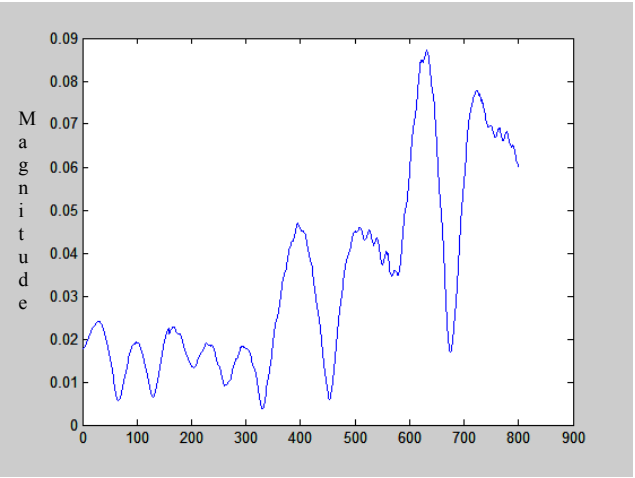

Frequency Range of 45MHz – 10GHz
Divided into 801 equal points

(c)

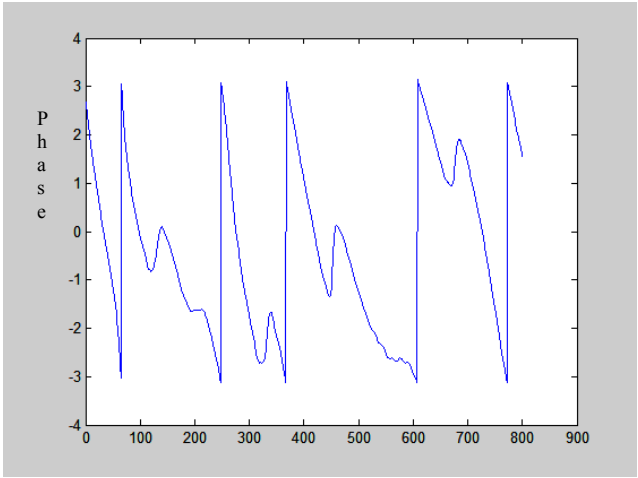

Frequency Range of 45MHz – 10GHz
Divided into 801 equal points

(d)

Figure 5.17: Reflection coefficients of the 20 dB attenuator and open standard: (c) magnitude at Port 2; and (d) phase at Port 2.

The following section presents the results from the TRL calibration using the three different devices under test.

5.3.2.1 TRL Calibration for an air filled transmission line

The entire procedure is again repeated with the air filled transmission line connected between the two fixtures along with the data for the modified short and open standard along with the 20 dB attenuator. As observed in Figures 5.16 and 5.17, because of the 20 dB attenuator, the reflection coefficient seen for the short ad open standards are no longer close to one. As per our assumption, with this combination of attenuator and standard, selecting a match standard will yield the same accuracy as short or open standard with the 20 dB attenuator. This is verified by observing the calculated reflection coefficients from the TRL deembedding algorithm as shown in Figures 5.18-5.20 in the next pages.

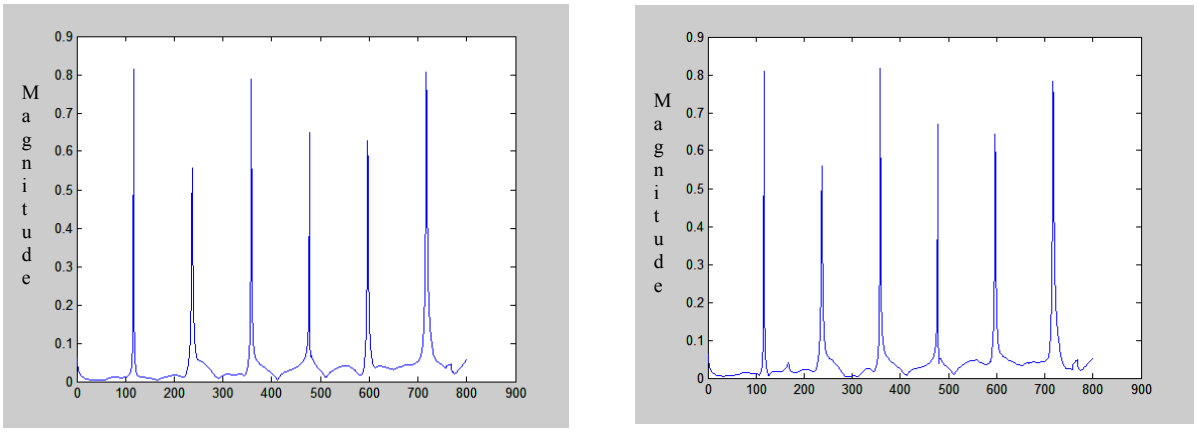

Frequency Range of 45MHz – 10GHz
Divided into 801 equal points
(a)

Frequency Range of 45MHz – 10GHz
Divided into 801 equal points
(b)

Figure 5.18: Calculated reflection coefficient from TRL algorithm for air filled transmission line: (a) match standard at Port 1; (b) match standard at Port 2.

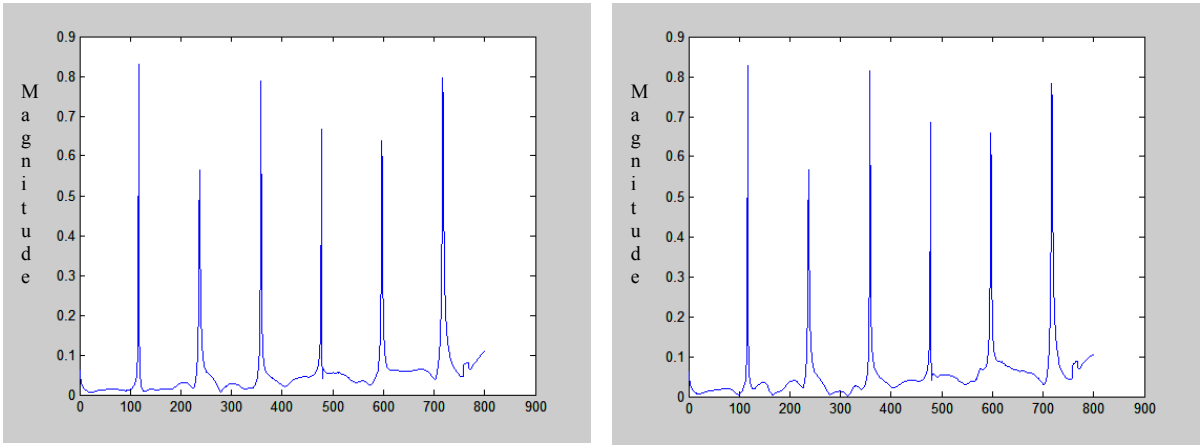

Frequency Range of 45MHz – 10GHz
Divided into 801 equal points
(a)

Frequency Range of 45MHz – 10GHz
Divided into 801 equal points
(b)

Figure 5.19: Calculated reflection coefficient from TRL algorithm for air filled transmission line: (a) open and 20 dB attenuator standard at Port 1; (b) open and 20 dB attenuator standard at Port 2.

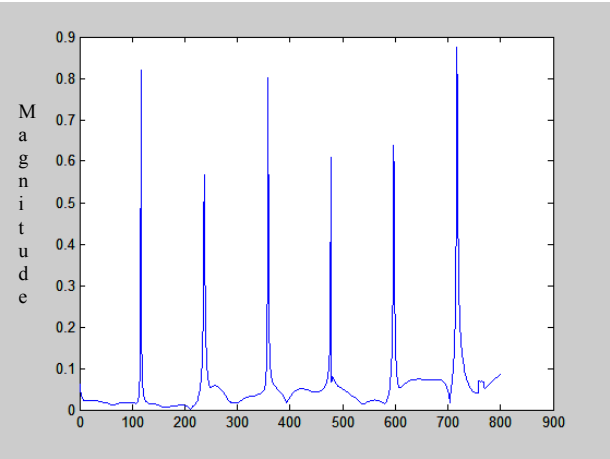

Frequency Range of 45MHz – 10GHz
Divided into 801 equal points

(a)

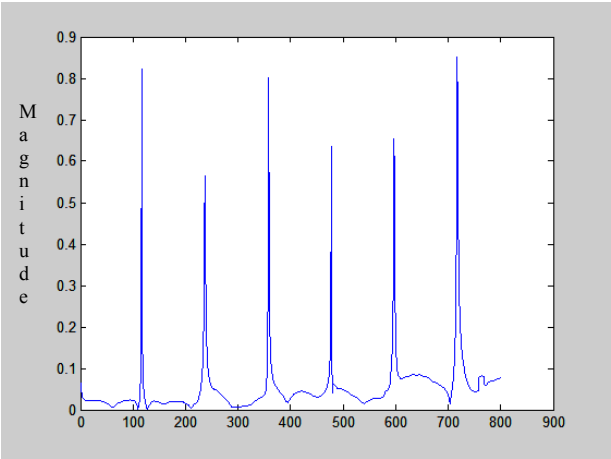

Frequency Range of 45MHz – 10GHz
Divided into 801 equal points

(b)

Figure 5.20: Calculated reflection coefficient from TRL algorithm for air filled transmission line: (a) short and 20 dB attenuator standard at Port 1; (b) short and 20 dB attenuator standard at Port 2.

Taking the error factor into consideration, as expected for all the three standards, namely the match, 20 dB attenuator with short/open standard should yield almost similar variation in the error factor. This observation is seen in Figure 5.21 below and in the next page.

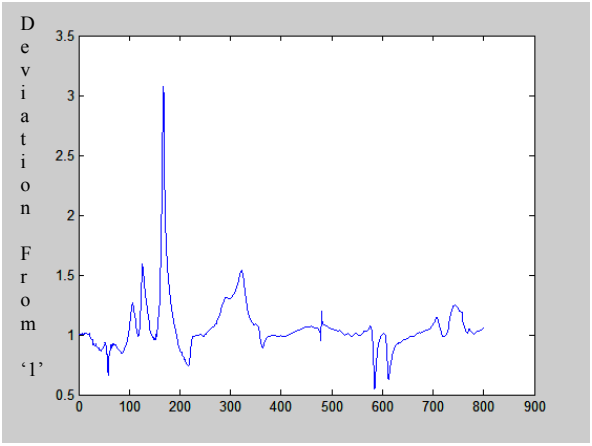

Frequency Range of 45MHz – 10GHz
Divided into 801 equal points

(a)

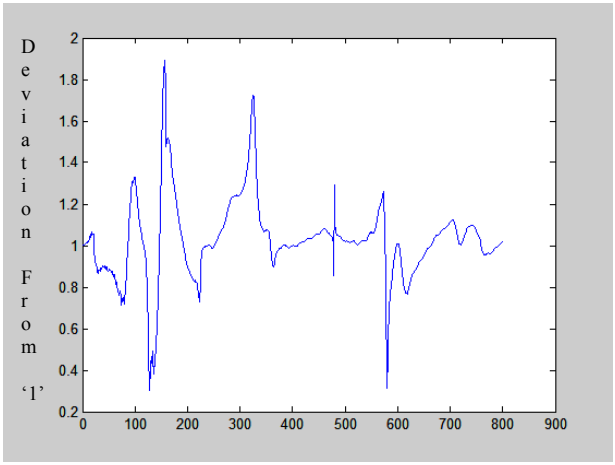

Frequency Range of 45MHz – 10GHz
Divided into 801 equal points

(b)

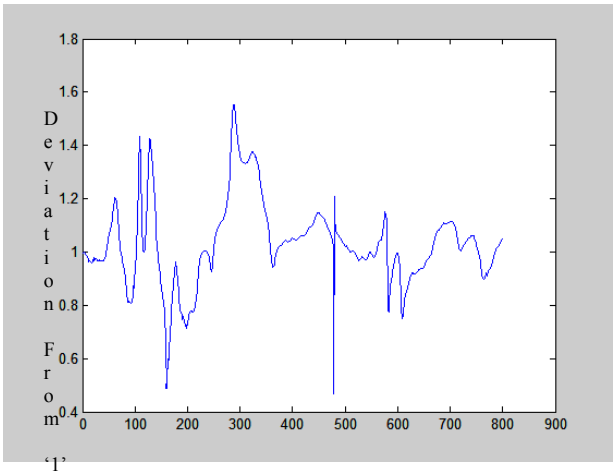

Frequency Range of 45MHz – 10GHz
Divided into 801 equal points

(c)

Figure 5.21: Error factor for different loads used in TRL procedure for the air filled transmission line with: (a) match standard; (b) 20 dB and open standard; (c) 20 dB and short standard.

5.3.2.2 TRL Calibration for a 20 dB attenuator

The entire procedure is again repeated with the air filled transmission line connected between the two fixtures replaced by a 20 dB attenuator along with the data obtained for the modified short and open standard along with the 20 dB attenuator. The calculated reflection coefficients from the TRL deembedding algorithm are shown in Figures 5.22-5.24 below.

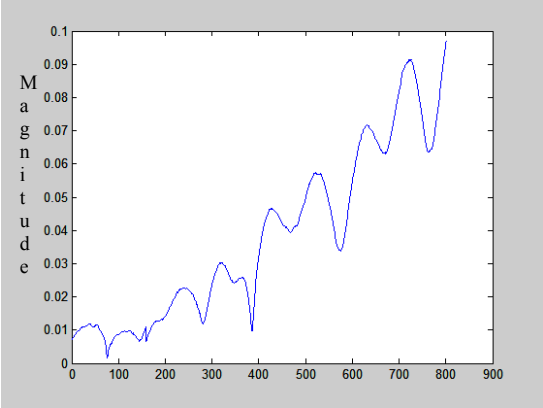

(a)

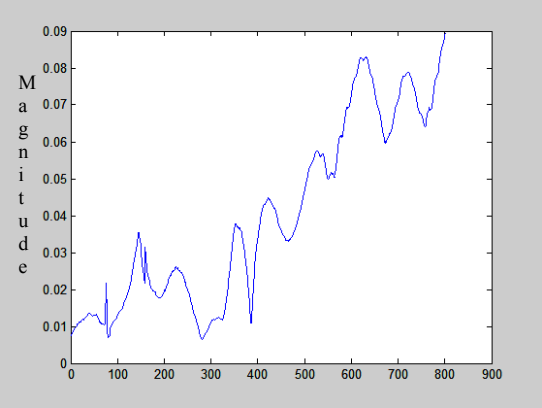

(b)

Figure 5.22: Calculated reflection coefficient from TRL algorithm for 20 dB attenuator: (a) match standard at Port 1; (b) match standard at Port 2.

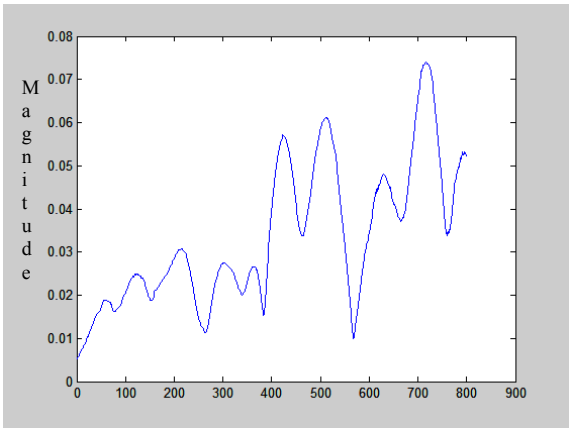

Frequency Range of 45MHz – 10GHz
Divided into 801 equal points

(a)

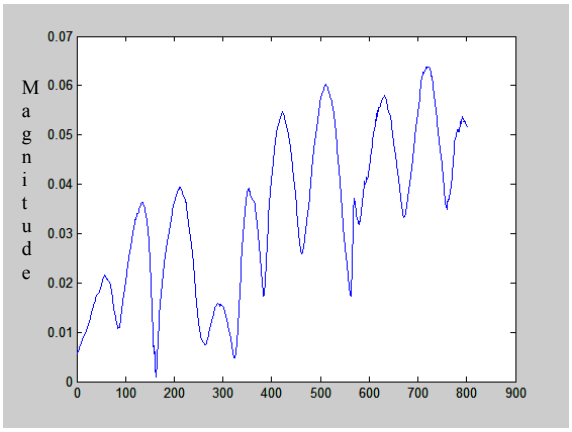

Frequency Range of 45MHz – 10GHz
Divided into 801 equal points

(b)

Figure 5.23: Calculated reflection coefficient from TRL algorithm for 20 dB attenuator: (a) open and 20 dB attenuator standard at Port 1; (b) open and 20 dB attenuator standard at Port 2.

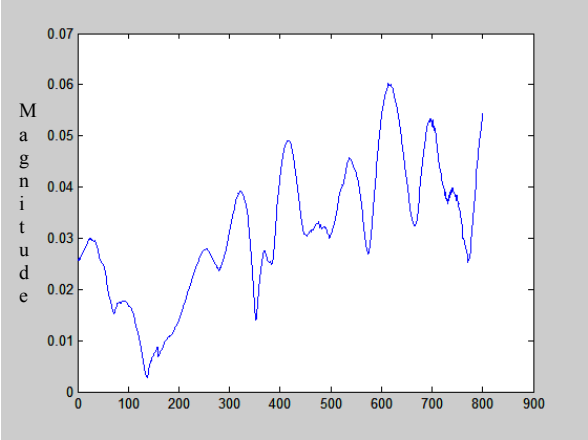

Frequency Range of 45MHz – 10GHz
Divided into 801 equal points

(a)

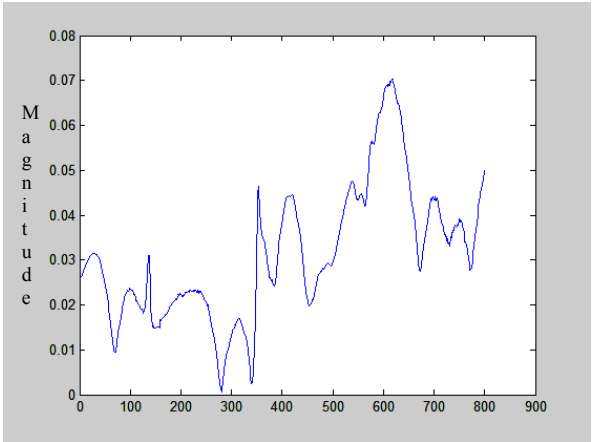

Frequency Range of 45MHz – 10GHz
Divided into 801 equal points

(b)

Figure 5.24: Calculated reflection coefficient from TRL algorithm for 20 dB attenuator: (a) short and 20 dB attenuator standard at Port 1; (b) short and 20 dB attenuator standard at Port 2.

Taking the error factor into consideration, as expected for all the three standards, namely the match and 20 dB attenuator with short/open standard should yield almost similar variation in the error factor. This observation is seen in Figure 5.25 below.

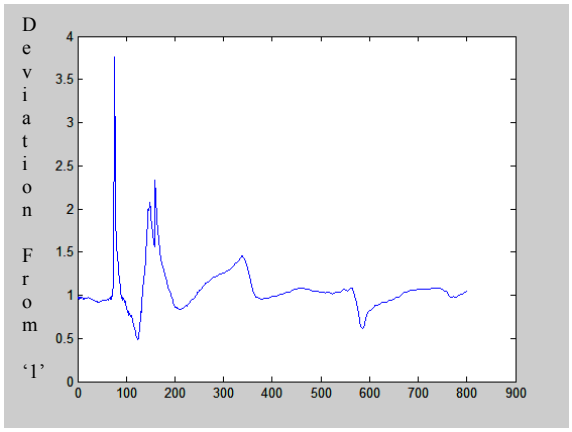

Frequency Range of 45MHz – 10GHz
Divided into 801 equal points

(a)

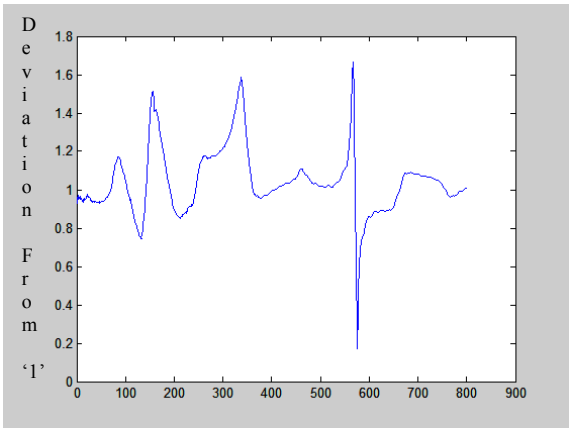

Frequency Range of 45MHz – 10GHz
Divided into 801 equal points

(b)

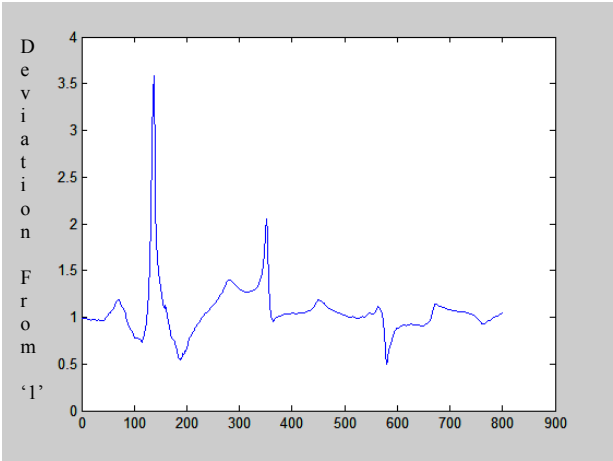

Frequency Range of 45MHz – 10GHz
Divided into 801 equal points

(c)

Figure 5.25: Error factor for different loads used in TRL procedure for the 20dB attenuator line with: (a) match standard; (b) open and 20 dB attenuator standard; (c) short and 20 dB attenuator standard.

5.3.2.3 TRL Calibration for a combination of 20dB attenuator and air filled transmission line

The entire procedure is again repeated with the 20 dB attenuator replaced by a 20db attenuator and an air filled transmission line along with the data obtained for the modified short and open standard along with the 20 dB attenuator. The calculated reflection coefficients from the TRL deembedding algorithm are shown in Figures 5.26-5.28 below.

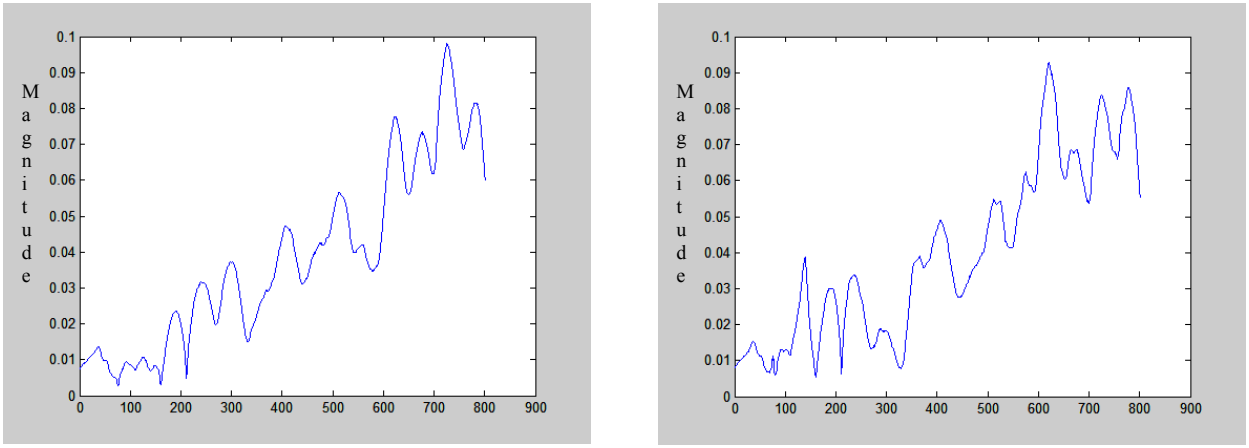

Figure 5.26: Calculated reflection coefficient from TRL algorithm for 20 dB attenuator and air filled transmission line for: (a) match standard at Port 1; (b) match standard at Port 2

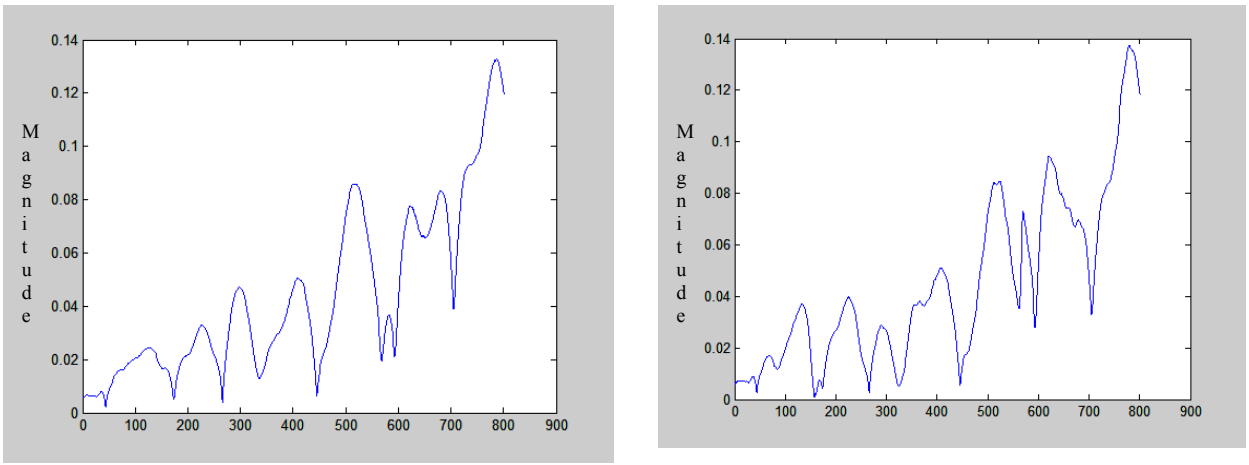

Frequency Range of 45MHz – 10GHz
Divided into 801 equal points

(a)

Frequency Range of 45MHz – 10GHz
Divided into 801 equal points

(b)

Figure 5.27: Calculated reflection coefficient from TRL algorithm for 20 dB attenuator and air filled transmission line for: (a) open and 20 dB attenuator standard at Port 1; (b) open and 20 dB attenuator standard at Port 2.

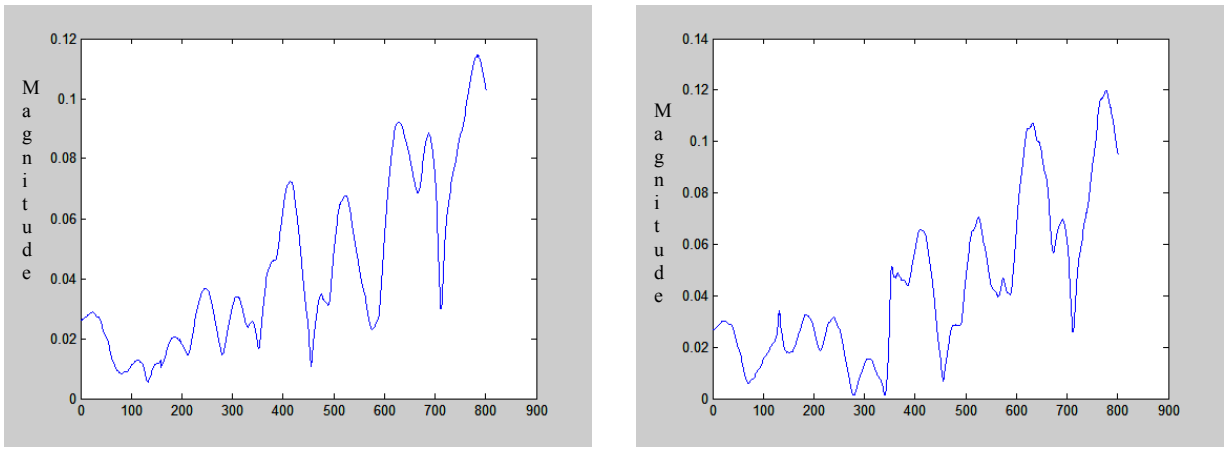

Frequency Range of 45MHz – 10GHz
Divided into 801 equal points

(a)

Frequency Range of 45MHz – 10GHz
Divided into 801 equal points

(b)

Figure 5.28: Calculated reflection coefficient from TRL algorithm for 20 dB attenuator and air filled transmission line for: (a) short and 20 dB attenuator standard at Port 1; (b) short and 20 dB attenuator standard at Port 2.

Taking the error factor into consideration, as expected for all the three standards, namely the match, 20 dB attenuator with short/open standard should yield almost similar variation in the error factor. This observation is seen in Figure 5.29 below.

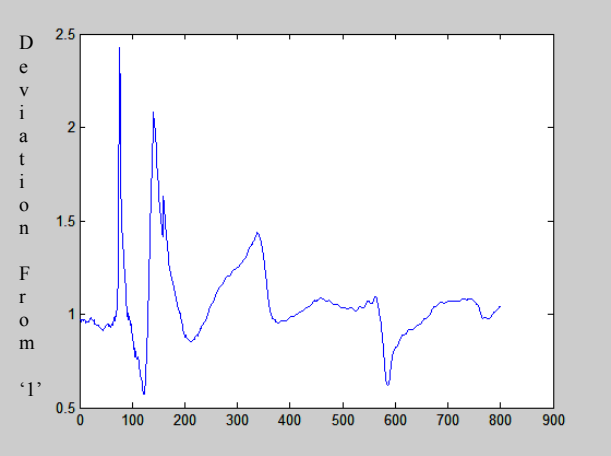

Frequency Range of 45MHz – 10GHz
Divided into 801 equal points

(a)

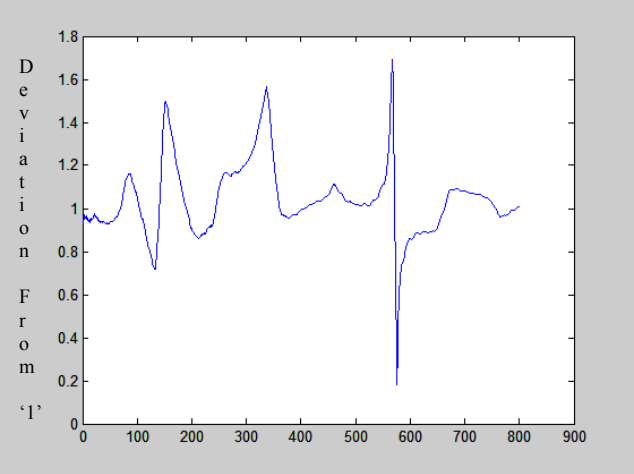

Frequency Range of 45MHz – 10GHz
Divided into 801 equal points

(b)

Figure 5.29: Error factor for different loads used in TRL procedure for the 20dB attenuator and air filled transmission line with: (a) match standard; (b) open and 20 dB attenuator standard.

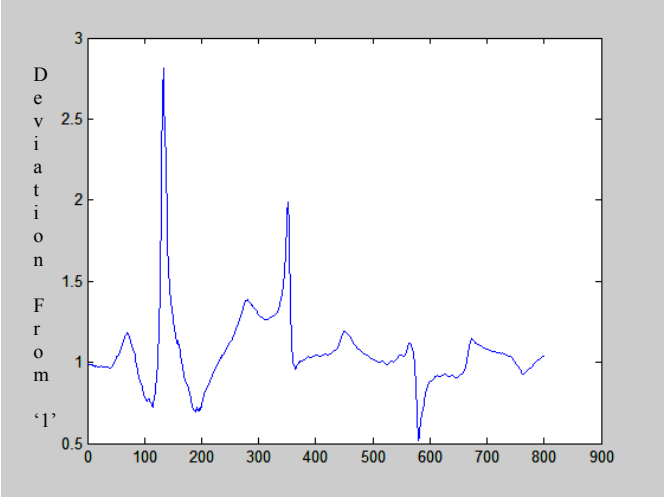

(c)

Figure 5.29: Error factor for different loads used in TRL procedure for the 20dB attenuator and air filled transmission line with: (c) short and 20 dB attenuator standard.

5.3.2.4 Comparison of results from TRL Calibration for the three devices with the 20 dB attenuator connected to the short and open standard

As seen from the experimental results, the error factor introduced in the TRL calibration for an air filled transmission line (as seen from Figure 5.21), for a 20dB attenuator (as seen from Figure 5.25) and for the combination of 20db attenuator and airline (as seen from Figure 5.29) show similar results, that is the error factor in all the three cases show same variation for short, open and match reflection standard because the addition of a 20dB attenuator reduces the reflection coefficient of the open and short standards near to zero thereby making the reflection coefficient value comparable to that of the match standard.

Chapter 6: Conclusions

From the presented work, an important conclusion has been drawn on the selection of the reflection standard required for accurate measurements. Apart from discussing the theoretical analysis of the discrepancies caused due to variation in the reflection coefficient seen at the two ports of the network analyzer, these discrepancies have been verified and proved experimentally as well. From the experimental analysis, it is also seen that similar variations in the measured data is obtained for TRL calibration on three different test devices to further prove the validity of the analysis. The final conclusion drawn is that the selection of short and open standard as the arbitrary reflection standard in TRL calibration procedure will yield the highest accuracy and the selection of match as the reflection standard will result in maximum inaccuracies in the final measurements.

References

[1] G. F. Engen and C. A. Hoer, **"Thru-refiect-line: an improved technique for calibrating the dual six-port automatic network analyzer,"** IEEE Trans. Microwave Theory Tech., vol. MTT-27, no. 12, pp. 987-993, December 1979.

[2] J. P. Mondal and T. H. Chen, **"Propagation constant determination in microwave fixture de-embedding procedure,"** IEEE Trans. Microwave Theory Tech., vol. MTT-36, no. 4, pp. 706-714, April 1988.

[3] M. B. Steer, S. B. Goldberg, G. Rinnet, P. D. Franzon, I. Turlik and J. S. Kasten, **"Introducing the Through-Line Deembedding Procedure,"** Microwave Symposium Digest, 1992., IEEE MTT-S International , 1-5 Jun 1992 Page(s):1455 -1458 vol.3.

[4] S.B. Goldberg, M.B. Steer, P.D. Franzon and J.S Kasten, "**Experimental electrical characterization of high speed interconnects,"** Electronic Components and Technology Conference, 1991. Proceedings., 41st , 11-16 May1991 Page(s): 85 -88.

[5] S.B. Goldberg, M.B. Steer, P.D. Franzon and J.S Kasten, "**Experimental electrical characterization of interconnects and discontinuities in high-speed digital systems,**" Components, Hybrids, and Manufacturing Technology, IEEE Transactions on [see also IEEE Trans. on Components, Packaging, and Manufacturing Technology, Part A, B, C] , Volume: 14 Issue:4 Dec 1991 Page(s):761 -765.

[6] M.B. Steer, J.S Kasten and R. Pomerleau, "**Enhanced through-reflect-line characterization of two-port measuring systems using free-space capacitance calculation,**" Microwave Theory and Techniques, IEEE Transactions on ,Volume: 38 Issue: 2 , Feb 1990 Page(s): 215 -217.

[7] H.P Application Note 1287-1**, "Understanding the Fundamental Principles of Vector Network Analysis".**

[8] http://www.ee.surrey.ac.uk

[9] H.P Application Note AN 1287-3, **"Applying Error Correction to Network Analyzer Measurements".**

[10] Characterization Handbook 1VNACAL.doc | 22.04.02 Franz Sischka.

[11] N. R. Franzen and R. A. Spaciale**, "A new procedure for system calibration and error removal in automated s-parameter measurements,"** Proc. 5th European Microwave Conf., pp. 69-73, 1975.

[12] H.P Product Note PN 8720-2, **"In-fixture Microstrip Device Measurements Using TRL Calibration".**

[13] Jeffery S. Kasten, **“Calibration of Automatic Network Analysis and Computer Aided Microwave Measurement,”** Masters thesis, 1992.

[14] Dylan Williams, **"De-embedding and Unterminating Microwave Fixtures with Nonlinear Least Squares,"** IEEE Trans. Microwave Theory Tech., vol. MTT-38, no. 6, pp. 787-791, June 1990.

[15] C. A. Hoer, **"Performance of a Dual Six-port Automatic Network Analyzer,"** IEEE Trans. Microwave Theory Tech., vol. MTT-27, no. 12, pp. 993-998, December 1979.

[16] R. B. Marks, **"A Multiline Method of Network Analyzer Calibration,"** IEEE Trans. Microwave Theory Tech., vol. MTT-39, no. 7, pp. 1205-1215, July 1991.

[17] D. F. Williams, R. B. Marks and A. Davidson, **"Comparison of On-wafer Calibrations,"** 38th ARFTG Conf. Dig., pp. 68-81, Dec 1991.

[18] R. F. Kaiser and D. F. Williams, **"Sources of Error in Coplanar-Waveguide TRL Calibrations,"** National Institute of Standards and Technology.

Appendix A

Detailed TRL De-Embedding Solution

The calibration procedure consists of measuring the S matrices for the three standards, namely Through, Reflect and Line which gives three known matrices. The three matrices obtained give the scattering parameters of the fictitious two ports and the scattering parameters of the individual error boxes A and B. The emergent wave amplitudes b_1, b_2 at ports 1 and 2 are related to the incident waves a_1, a_2 by the well-known scattering equations:

$$b_1 = S_{11}a_1 + S_{12}b_2 \tag{A.1}$$

$$b_2 = S_{21}a_1 + S_{22}b_2 \tag{A.2}$$

where the S_{ij} are the scattering coefficients.

Dividing the first of these by a_1, the second by a_2, and then eliminating the ratio a_1/a_2 between them yields:

$$w_2S_{11} + w_2S_{22} - \Delta = w_1w_2 \tag{A.3}$$

where

$$\Delta = S_{11}S_{22} - S_{12}S_{21} \tag{A.4}$$

The equation (3.5) shows the conversion between the T and the S parameters.

$$\begin{bmatrix} R_{11} & R_{12} \\ R_{21} & R_{22} \end{bmatrix} = \begin{bmatrix} -\dfrac{S_{11}S_{22} - S_{12}S_{11}}{S_{21}} & \dfrac{S_{11}}{S_{21}} \\ -\dfrac{S_{22}}{S_{21}} & \dfrac{1}{S_{21}} \end{bmatrix} \tag{A.5}$$

First convert the measured S parameters to their equivalent T parameters as in equation (A.5). Let the cascading matrix be represented by the matrix R. Let the cascading matrices of the error two-ports A and B be denoted by R_a and R_b

respectively, while R_t represents their cascade 'thru' connection and R_d represents the cascade 'Line' measurements and R_l represents the cascade matrix of the inserted line.

Then

$$R_t = R_a R_b \tag{A.6}$$

and,

$$R_d = R_a R_{l2} R_b \tag{A.7}$$

Solving (A.6) to get

$$R_b = R_a^{-1} R_t \tag{A.8}$$

Hence error matrix R_b can be obtained from the above equation.

Eliminating R_b in equation (A.6) we obtain the following

$$TR_a = R_a R_{l2}$$

Where: $T = R_d R_t^{-1}$ (A.9)

or

$$\begin{bmatrix} t_{11} & t_{12} \\ t_{21} & t_{22} \end{bmatrix} = \begin{bmatrix} r_{11M1} & r_{12M1} \\ r_{21M1} & r_{22M1} \end{bmatrix} \begin{bmatrix} r_{11M2} & r_{12M2} \\ r_{21M2} & r_{22M2} \end{bmatrix}^{-1}$$

Where T matrix is represented by: $\mathbf{T} = \begin{bmatrix} t_{11} & t_{12} \\ t_{21} & t_{22} \end{bmatrix}$ (A.10)

R_d matrix is represented by: $\mathbf{R_d} = \begin{bmatrix} r_{11M2} & r_{12M2} \\ r_{21M2} & r_{22M2} \end{bmatrix}$ (A.11)

and R_t matrix is represented by: $\mathbf{R_t} = \begin{bmatrix} r_{11M1} & r_{12M1} \\ r_{21M1} & r_{22M1} \end{bmatrix}$ (A.12)

Let R_a matrix be represented by: $\mathbf{R_a} = \begin{bmatrix} r_{11a} & r_{12a} \\ r_{21a} & r_{22a} \end{bmatrix}$

or $\mathbf{R_a} = r_{22a} \begin{bmatrix} a & b \\ c & 1 \end{bmatrix}$ (A.13)

where $a = r_{11a} / r_{22a}$, $b = r_{12a} / r_{22a}$ and $c = r_{21a} / r_{22a}$.

Let R_b matrix be represented by: $\mathbf{R_b} = \begin{bmatrix} r_{11b} & r_{12b} \\ r_{21b} & r_{22b} \end{bmatrix}$

or $\mathbf{R_b} = r_{22b} \begin{bmatrix} \alpha & \beta \\ \gamma & 1 \end{bmatrix}$ (A.14)

where $\alpha = r_{11b} / r_{22b}$, $\beta = r_{12b} / r_{22b}$ and $\gamma = r_{21b} / r_{22b}$.

Hence equation (A.9) can also be written as

$$\mathbf{T} = \begin{bmatrix} t_{11} & t_{12} \\ t_{21} & t_{22} \end{bmatrix} = \begin{bmatrix} r_{11M1} & r_{12M1} \\ r_{21M1} & r_{22M1} \end{bmatrix} \begin{bmatrix} r_{11M2} & r_{12M2} \\ r_{21M2} & r_{22M2} \end{bmatrix}^{-1} \quad \text{(A.15)}$$

Assuming that the line (represented by ℓ_2) in non-reflecting, matrix R_d changes to

$$\mathbf{R_d} = \begin{bmatrix} r_{11M1} & r_{12M1} \\ r_{21M1} & r_{22M1} \end{bmatrix} = \begin{bmatrix} eExp(-\gamma l 2) & 0 \\ 0 & eExp(\gamma l 2) \end{bmatrix}$$

Substituting the above mentioned matrix in equation (A.9) yields the following four sets of equation:

$$t_{11a} r_{11a} + t_{12a} r_{21a} = r_{11a} e^{-\gamma l} \quad \text{(A.16)}$$

$$t_{21a} r_{11a} + t_{22a} r_{21a} = r_{21a} e^{-\gamma l} \quad \text{(A.17)}$$

$$t_{11a} r_{12a} + t_{12a} r_{22a} = r_{12a} e^{-\gamma l} \quad \text{(A.18)}$$

$$t_{21a} r_{12a} + t_{22a} r_{22a} = r_{22a} e^{-\gamma l} \quad \text{(A.19)}$$

Taking ratio of equation (A.16) to (A.17) and equation (A.18) to (3.19) yields

$$t_{21a}(r_{11a} / r_{11a})^2 + (t_{22a} - t_{11a})(r_{11a} / r_{11a}) - t_{12a} = 0 \quad \text{(A.20)}$$

$$t_{21a}(r_{12a} / r_{22a})^2 + (t_{22a} - t_{11a})(r_{12a} / r_{22a}) - t_{12a} = 0 \quad \text{(A.21)}$$

Ratio of equation (A.19) to (A.17) yields

$$e\,\mathrm{Exp}\,(2\gamma\ell) = \frac{t_{21a}(r_{12a}/r_{22a}) + t_{22a}}{t_{12a}(r_{21a}/r_{11a}) + t_{11a}} \tag{A.22}$$

Hence from equations (A.20), (A.21) and (A.22), we have obtained three quantities:

$$a/c = (r_{11a}/r_{21a})\ ,\ b = (r_{12a}/r_{22a})$$

and $$e\,\mathrm{Exp}\,(2\gamma\ell) = \frac{t_{21a}(r_{12a}/r_{22a}) + t_{22a}}{t_{12a}(r_{21a}/r_{11a}) + t_{11a}} \tag{A.23}$$

The reflection coefficient w_1 obtained at the fictitious port for the two port error A is related to the reflection coefficient of the load by

$$w_1 = \frac{a\Gamma_l + b}{c\Gamma_l + 1} \tag{A.24}$$

or

$$a = \frac{w_1 - b}{\Gamma_l(1 - w_1 * c/a)} \tag{A.25}$$

Similar analysis on the second two port error B yields

$$w_2 = \frac{\alpha\Gamma_l - \gamma}{-\beta\Gamma_l + 1} \tag{A.26}$$

or

$$\alpha = \frac{w_2 - \gamma}{\Gamma_l(1 + w_2 * \beta/\alpha)}\,. \tag{A.27}$$

The unknown reflection coefficient Γ_l is eliminated from equation (A.25) and (A.27) to yield

$$a = \pm\sqrt{[(w_1 - b)(1 + w_2\beta/\alpha)(d - bf)]/[(w_2 + \gamma c/a)(1 - ec/a)]} \tag{A.28}$$

Thus the need for the value of reflection coefficient to be exactly known is eliminated.

Once the value for 'a' for two port error matrix A is found, the remaining parameters of the equation (A.13) and (A.14) can be found as follows:

From the 'Thru' and 'Line' measurements (A.23), the values for b and a/c have already been obtained. Then from (A.6) substituting the matrix we get

$$r_{22a}\begin{bmatrix} a & b \\ c & 1 \end{bmatrix} * r_{22b}\begin{bmatrix} \alpha & \beta \\ \gamma & 1 \end{bmatrix} = g\begin{bmatrix} d & e \\ f & 1 \end{bmatrix} \tag{A.29}$$

where:

$$g\begin{bmatrix} d & e \\ f & 1 \end{bmatrix} = r_{22M1}\begin{bmatrix} r_{11M1}/r_{22M1} & r_{12M1}/r_{22M1} \\ r_{21M1}/r_{22M1} & 1 \end{bmatrix}$$

From (A.29) the following parameters can be easily obtained

$$\gamma = \frac{f - dc/a}{1 - ec/a} \tag{A.30}$$

$$\beta/\alpha = \frac{e - b}{d - bf} \tag{A.31}$$

$$a\alpha = \frac{d - bf}{1 - ec/a} \tag{A.32}$$

Hence from the above set of equations all the parameters of the 2 sets of error matrix A and B can be found out. This entire procedure sums up the TRL solution for de-embedding.

Appendix B

MATLAB Code for TRL Deembedding

```
% MATLAB Code for TRL Deembedding Solution
% Author: Rahul Ghosh

% Step 1: Reading Frequency for the Different Samples
fid = fopen('frequency.txt','rt');
af = fscanf(fid,'%f',[1,900])'
fclose(fid)

% Step 2: Reading S Measurements for Through Standard

fid = fopen('c_thru.txt','rt');
a9 = fscanf(fid,'%f %f',[2,3204])'
fclose(fid)

for i = 1:3204
   a9_com(i) = complex(a9(i,1),a9(i,2));
end

% Storing the S11 parameters for different frequencies
for i = 1:801
   S(1,i) = a9_com(i);

end

% Storing the S12 parameters for different frequencies
for i = 1:801
   S(2,i) = a9_com(1602+i);
end

% Storing the S21 parameters for different frequencies
for i = 1:801
   S(3,i) = a9_com(801+i);
end

% Storing the S22 parameters for different frequencies
for i = 1:801
   S(4,i) = a9_com(2403+i);
end
```

% Step 3: Convert reading from S to T parameters for further processing.

```
% S11 conversion
for i = 1:801
  Rt1_t(1,i) = -((S(1,i)* S(4,i) - S(2,i)*S(3,i))/S(3,i))
end

% S12 conversion
for i = 1:801
   Rt1_t(2,i) = S(1,i)/S(3,i)
end

% S21 conversion
for i = 1:801
   Rt1_t(3,i) = - S(4,i)/S(3,i)
end

% S22 conversion
for i = 1:801
   Rt1_t(4,i) = 1/S(3,i)
end
```

% Step 4: Reading files for different sets of measurements and storing them
% appropriately.

```
fid = fopen('20db_attn_line.txt','rt');

b1 = fscanf(fid,'%f %f',[2,3204])'
fclose(fid)

for i = 1:3204
   b1_com(i) = complex(b1(i,1),b1(i,2));
end
for i = 1:801
   S1(1,i) = b1_com(i);
end
for i = 1:801
   S1(2,i) = b1_com(1602+i);
end
for i = 1:801
   S1(3,i) = b1_com(801+i);
end
for i = 1:801
   S1(4,i) = b1_com(2403+i);
end
```

% Convert from S to T parameters for further processing

```
% S11 conversion
for i = 1:801
   Rd_t(1,i) = -((S1(1,i)* S1(4,i) - S1(2,i)*S1(3,i))/S1(3,i))
end

% S12 conversion
for i = 1:801
   Rd_t(2,i) = S1(1,i)/S1(3,i)
end

% S21 conversion
for i = 1:801
   Rd_t(3,i) = - S1(4,i)/S1(3,i)
end

% S22 conversion
for i = 1:801
   Rd_t(4,i) = 1/S1(3,i)
end
```

% Reading files for Matched load for side 1

```
fid = fopen('c_m1.txt','rt');
a1 = fscanf(fid,'%f %f',[2,900])'
fclose(fid)
for i = 1:801
   a1_com(i) = complex(a1(i,1),a1(i,2));
end
for i = 1:801
   Sm(1,i) = a1_com(i);
end
```

% Reading files for Matched load for side 2

```
fid = fopen('c_m2.txt','rt');
a2 = fscanf(fid,'%f %f',[2,900])'
fclose(fid)
for i = 1:801
   a2_com(i) = complex(a2(i,1),a2(i,2));
end
for i = 1:801
   Sm2(1,i) = a2_com(i);
end
```

% Reading files for SHORT load for side 1

```
fid = fopen('s501.txt','rt');
a3 = fscanf(fid,'%f %f',[2,900])'
fclose(fid)
for i = 1:801
```

```
   a3_com(i) = complex(a3(i,1),a3(i,2));
end
for i = 1:801
   Ss1(1,i) = a3_com(i);
end
```

% Reading files for SHORT load for side 2

```
fid = fopen('s502.txt','rt');
a4 = fscanf(fid,'%f %f',[2,900])'
fclose(fid)
for i = 1:801
   a4_com(i) = complex(a4(i,1),a4(i,2));
end
for i = 1:801
   Ss2(1,i) = a4_com(i);
end
```

% **Reading files for OPEN load for side 1**

```
fid = fopen('o501.txt','rt');
a5 = fscanf(fid,'%f %f',[2,900])'
fclose(fid)
for i = 1:801
   a5_com(i) = complex(a5(i,1),a5(i,2));
end
for i = 1:801
   So1(1,i) = a5_com(i);
end
```

% Reading files for OPEN load for side 2

```
fid = fopen('o502.txt','rt');
a6 = fscanf(fid,'%f %f',[2,900])'
fclose(fid)
for i = 1:801
   a6_com(i) = complex(a6(i,1),a6(i,2));
end
for i = 1:801
   So2(1,i) = a6_com(i);
end
```

% Step 5: Begin TRL Deembedding algorithm according to [1].

```
i = 1
while (i <= 801)
   for j=1:2
     for k =1:2
       Rt1(j,k) = Rt1_t((j-1)*2+k,i)
       Rd(j,k)  = Rd_t((j-1)*2+k,i)
      end
   end
```

```
  RM1_s(i) = Sm(1,i)
  RM2_s(i) = Sm2(1,i)
  RS1_s(i) = Ss1(1,i)
  RS2_s(i) = Ss2(1,i)
  Ro1_s(i) = So1(1,i)
  Ro2_s(i) = So2(1,i)


% Calculation of the reflection coefficient ‘w1 and w2’ for the calculation of 'a'
% Refer to w1 and w2 in [1]

% For MATCH standard
  rc_m1(i) = RM1_s(i)   % w1
  rc_m2(i) = RM2_s(i)   % w2

  rc_m1_mag(i) = abs(rc_m1(i))
  rc_m2_mag(i) = abs(rc_m2(i))

  rc_m1_phase(i) = angle(rc_m1(i))
  rc_m2_phase(i) = angle(rc_m2(i))

% For SHORT standard
  rc_s1(i) = RS1_s(i)
  rc_s2(i) = RS2_s(i)

  rc_s1_phase(i) = angle(rc_s1(i))
  rc_s2_phase(i) = angle(rc_s2(i))

  rc_s1_mag(i) = abs(rc_s1(i))
  rc_s2_mag(i) = abs(rc_s2(i))


% For OPEN standard
   rc_o1(i) = Ro1_s(i)
   rc_o2(i) = Ro2_s(i)
   rc_o1_mag(i) = abs(rc_o1(i))
   rc_o2_mag(i) = abs(rc_o2(i))

   rc_o1_phase(i) = angle(rc_o1(i))
   rc_o2_phase(i) = angle(rc_o2(i))

% Further processing, please refer [1]
  T = Rd * inv(Rt1)

% Storing the data for solving the quadratic equation.

  a_eq(i) = T(2,1)
  b_eq(i) = (T(2,2) - T(1,1))
  c_eq(i) = T(1,2)
```

```
% Calculating the roots for solving the quadratic equation.
 root1(i) = (((-b_eq(i))+(((b_eq(i)^2)-(4*a_eq(i)*c_eq(i)))^(1/2)))/(2*a_eq(i)))
 root2(i) = (((-b_eq(i))-(((b_eq(i)^2)-(4*a_eq(i)*c_eq(i)))^(1/2)))/(2*a_eq(i)))

% Selecting the right roots values for which abs (b) < abs (a/c)
 root1_mag(i) = abs(root1(i)) % = 0.4449
 root2_mag(i) = abs(root2(i)) % = 2.5931


 if (root1_mag(i)  < root2_mag(i))
   b(i) = root1(i)
   a_c(i) = root2(i)
 else
   b(i) = root2(i)
   a_c(i) = root1(i)
 end


% Removing the 'through 22' element outside the matrix
Rt  = Rt1/Rt1(2,2) % Rt 'one'


% Calculations for the error box B
% Notations same as those used in [1]
d(i) = Rt(1,1)
e(i) = Rt(1,2)
f(i) = Rt(2,1)


gamma(i) = (f(i) - (d(i)*(1/a_c(i))))/(1 - e(i)*(1/a_c(i)))
beta_alpha(i) = (e(i) - b(i))/(d(i)-(b(i)*f(i)))
a_alpha(i) = (d(i) - (b(i)*f(i)))/(1-(e(i)*(1/a_c(i))))


% Estimation in the value of 'a' for different loads

% For Match condition
a_matched_wo_error(i) = sqrt(((rc_m1(i) - b(i))*(1 + rc_m2(i)* beta_alpha(i))*(d(i) -
b(i)*f(i)))/((rc_m2(i) + gamma(i))*(1 - rc_m1(i)*(1/a_c(i)))*(1-e(i)*(1/a_c(i)))))

% For Short condition
a_short_wo_error(i) = sqrt(((rc_s1(i) - b(i))*(1 + rc_s2(i)* beta_alpha(i))*(d(i) -
b(i)*f(i)))/((rc_s2(i) + gamma(i))*(1 - rc_s1(i)*(1/a_c(i)))*(1-e(i)*(1/a_c(i)))))

% For Open condition
a_open_wo_error(i) = sqrt(((rc_o1(i) - b(i))*(1 + rc_o2(i)* beta_alpha(i))*(d(i) -
b(i)*f(i)))/((rc_o2(i) + gamma(i))*(1 - rc_o1(i)*(1/a_c(i)))*(1-e(i)*(1/a_c(i)))))
```

% Step 6: Calculations taking into considerations the proposed error factor

% First Estimate the variation in the value of Reflection Co-efficient seen at the two
% ports.

% To find the error value you will need to find the reflection coefficient 1 and 2 with
% values w1 and w2 and then subtract them to find error.

% Reflection co-efficient of side 1.

% For match standard
reflection_coef_m1(i) = ((rc_m1(i) - b(i))/(a_matched_wo_error(i)*(1 - (rc_m1(i)*1/a_c(i)))))

% For short standard
reflection_coef_s1(i) = ((rc_s1(i) - b(i))/(-a_short_wo_error(i)*(1 + (rc_s1(i)*1/a_c(i))))) % changed

% For open standard
reflection_coef_o1(i) = ((rc_o1(i) - b(i))/(a_open_wo_error(i)*(1 - (rc_o1(i)*1/a_c(i)))))

reflection_coef_m1_mag(i) = abs(reflection_coef_m1(i))
reflection_coef_s1_mag(i) = abs(reflection_coef_s1(i))
reflection_coef_o1_mag(i) = abs(reflection_coef_o1(i))

% Reflection co-efficient of side 2

% For match standard
reflection_coef_m2(i) = ((rc_m2(i) - b(i))/(a_matched_wo_error(i)*(1 - (rc_m2(i)*1/a_c(i)))))

% For short standard
reflection_coef_s2(i) = ((rc_s2(i) - b(i))/(-a_short_wo_error(i)*(1 + (rc_s2(i)*1/a_c(i)))))

% For open standard
reflection_coef_o2(i) = ((rc_o2(i) - b(i))/(a_open_wo_error(i)*(1 - (rc_o2(i)*1/a_c(i)))))

reflection_coef_m2_mag(i) = abs(reflection_coef_m2(i))
reflection_coef_s2_mag(i) = abs(reflection_coef_s2(i))
reflection_coef_o2_mag(i) = abs(reflection_coef_o2(i))

% Error factor calculations

% For match, short and open standards.

```
error_m(i) = (reflection_coef_m1(i) - reflection_coef_m2(i))
error_s(i) = (reflection_coef_s1(i) - reflection_coef_s2(i))
error_o(i) = (reflection_coef_o1(i) - reflection_coef_o2(i))
```

% The variation in the value of ‘a’ from the accurate measurement for different
% standards used, namely match, open and short.

```
a_varies_by_m(i) = sqrt(1+(error_m(i)/(reflection_coef_m1(i))))
a_varies_by_o(i) = sqrt(1+(error_o(i)/(reflection_coef_o1(i))))
a_varies_by_s(i) = sqrt(1+(error_s(i)/(reflection_coef_s1(i))))

a_varies_by_m_mag(i) = abs(a_varies_by_m(i))
a_varies_by_s_mag(i) = abs(a_varies_by_s(i))
a_varies_by_o_mag(i) = abs(a_varies_by_o(i))
```

% The value ‘i’ traverses through the 801 set of readings for different frequencies.

```
i=i+1

end
```